B7-H3-DIRECTED CHIMERIC ANTIGEN RECEPTOR T CELLS FOR THE TREATMENT OF GLIOBLASTOMA MULTIFORME

Dean Nehama

A dissertation submitted to the faculty at University of North Carolina at Chapel Hill in partial fulfillment of the requirements for the degree of Doctor of Philosophy in the Curriculum in Genetics and Molecular Biology in the UNC Graduate School.

Chapel Hill
2019

Approved by:

William Kim

Barbara Savoldo

Yue Xiong

Jason Whitmire

Shawn Hingtgen

ABSTRACT

Dean Nehama: B7-H3-directed chimeric antigen receptor T cells for the treatment of glioblastoma multiforme
(Under the direction of Barbara Savoldo)

Glioblastoma multiforme (GBM) has continued to pose an immense clinical challenge that, despite decades of research elucidating its complex tumor biology and development of various therapeutic modalities, still holds a grim survival to all patients. The molecular heterogeneity of GBM within and across tumors, as well as its immunosuppressive environments have been the most challenging obstacles to overcome in this disease, and so far they remain insurmountable. In this dissertation, I lay out advances this field has made in the understanding of the cell and microenvironmental biology of GBM, with particular emphasis on molecular and immunological heterogeneity, and in the therapeutic approaches for GBM. My colleagues and I show that chimeric antigen receptor (CAR) T cell therapy is particularly suited to make a difference in patients lives, assuming an appropriate antigen is targeted. We generated B7-H3-directed CAR T cells and demonstrate that they eliminate GBM cell lines and patient-derived GBM cells enriched with cancer stem cells across all GBM molecular subtypes both *in vitro* and *in vivo*. Our data indicates that B7-H3 is a particularly attractive antigen for this approach because of its ubiquitously high expression within and across most tumors. Given our results, we recommend that B7-H3-directed CAR T cells be investigated further for GBM treatment.

ACKNOWLEDGEMENTS

There have been many people that helped along the way throughout my journey in graduate school. It felt both like a particularly tumultuous journey and one full of opportunities – and definitely one full of transitions. As an MD-PhD student, transitioning from the structured curriculum of medical school to the ambiguous work schedule was initially confusing. It took me time to understand what I am supposed to do. I initially started as a student in the lab of Dr. Norman Sharpless, without much immunology background and without strong intent to pursue immunology, yet I was working on a project investigating the effect of *CDKN2A* deletion in T cells on aging and cancer in mice. When this project yielded disappointing results, I shifted to a T cell-based immunotherapy project, still at the Sharpless Lab. Soon after, Dr. Sharpless left UNC to head the National Cancer Institute, and I was fortunate to have been able to join the lab of Drs. Barbara Savoldo and Gianpietro Dotti, where I began yet another new project - the one described in this dissertation - in a field that I still felt was new to me. It was challenging, but I learned a lot. This graduate school experience, and the extracurricular opportunities surrounding it, have clarified to me why I love being in an academic environment. It is full of growth opportunities, curious and creative minds, and collaborative teams, all geared towards making a difference in people's lives.

I am grateful for the people that have been part of this journey: Thank you to the MD-PhD program at UNC for allowing me to pursue this opportunity. Thank you Dr.

Sharpless for taking me as your graduate student, introducing me to aging and cancer research, guiding me through my projects, and sharing your wisdom with me. Thank you to the members of the Sharpless lab for supporting me and mentoring me. Thank you Drs. Savoldo and Dotti for accepting me into your lab and giving me the opportunity to be part of the exciting field of CAR T therapy, and for your mentorship. Thank you to the members of the Savoldo/Dotti lab for training me on techniques in the field and fostering a supportive environment in the lab. Thank you Dr. Cyrus Vaziri for being a mentor to me throughout graduate school and an excellent instructor. Thank you to my dissertation committee, and especially my committee chair Dr. William Kim, for your guidance in my projects and your patience through my project transitions. Thank you to my family for being supportive of me in pursuing this long training opportunity so far away from home, and for continuing our annual family trip tradition so that we not only spend quality time together but also travel the world together. I am especially grateful for my sister Shir and for the fact that even though we live so far apart, we always remain close.

TABLE OF CONTENTS

LIST OF TABLES

LIST OF FIGURES

LIST OF ABBREVIATIONS

ADC:	Antibody-drug conjugate
ALL:	Acute lymphoblastic leukemia
BBB:	Blood-brain barrier
BLI:	Bioluminescence intensity
BSA:	Bovine serum albumin
CAR:	Chimeric antigen receptor
CD:	Cluster of differentiation
CFSE:	Carboxyfluorescein succinimidyl ester
CTLA-4:	Cytotoxic T-lymphocyte-associated protein 4
G-CIMP:	Glioblastoma CpG island methylator phenotype
CNS:	Central nervous system
CRS:	Cytokine release syndrome
CSC:	Cancer stem cell
CSF-1:	Colony stimulating factor 1
CSPG4:	Chondroitin sulphate proteoglycan 4
cT:	Control non-transduced T cells
CTL:	Cytotoxic lymphocyte
DC:	Dendritic cell
Depatux-M:	Depatuxizumab mafodotin
DISC:	Death-inducing signaling complex
DMEM:	Dulbecco modified eagle medium
EDTA:	Ethylenediaminetetraacetic acid
EGFR:	Epidermal growth factor receptor

EGFRvIII:	Epidermal growth factor receptor variant III
ELISA:	Enzyme-linked immunosorbent assay
EORTC:	European Organisation for Research and Treatment of Cancer
ER:	Endoplasmic reticulum
EphA2:	Ephrin type-A receptor 2
ErbB2:	Erythroblastic oncogene B 2
E:T:	Effector-to-target ratio
FDA:	Food and Drug Administration
FFLuc:	Firefly luciferase
FFPE:	Formalin-fixed paraffin-embedded
GBM:	Glioblastoma multiforme
GD2:	Disialoganglioside 2
GFP:	Green fluorescent protein
GM-CSF:	Granulocyte-macrophage colony-stimulating factor
HEPES:	(4-(2-hydroxyethyl)-1-piperazineethanesulfonic acid
HER2:	Human epidermal growth factor receptor 2
2-HG:	2-hydroxyglutarate
HLA:	Human leukocyte antigen
HSV:	Herpes simplex virus
HVEM:	Herpesvirus entry mediator
IACUC:	Institutional Animal Care and Use Committee
IDH:	Isocitrate dehydrogenase
IFN:	Interferon

IHC: Immunohistochemistry

IL: Interleukin

IL-13Rα2: Interleukin-13 receptor alpha 2

iNOS: Inducible nitric oxide synthase

ITAM: Immunoreceptor tyrosine-based activation motif

α-KG: α-ketoglutarate

Lck: Lymphocyte-specific protein tyrosine kinase

Mafodotin: Monomethyl auristatin F

MCP-1: Monocyte chemoattractant protein 1

MDM2: Mouse double minute 2 homolog

MDSC: Myeloid-derived suppressor cell

MHC: Major histocompatibility

MIC-1: Macrophage inhibitory cytokine 1

MGMT: O^6-methylguanine-methyltranseferase

MMAE: Monomethyl auristatin E

MOI: Multiplicity of infection

MRD: Minimal residual disease

mTOR: Mammalian target of rapamycin

Nck: Non-catalytic region of tyrosine kinase

NF1: Neurofibromatosis 1

NK: Natural killer

NO: Nitric oxide

NS: Neurosphere

pAPC: Professional antigen presenting cell

PBS: Phosphate-buffered saline

PDGF: Platelet-derived growth factor

PD-L1: Programmed death ligand 1

PFS: Progression-free survival

PI3K: phosphatidylinositol-3-OH kinase

PNT: Peroxynitrite

PTEN: Phosphatase and tensin homolog

RAG: Recombination activating gene

Rb: Retinoblastoma

RTK: Receptor tyrosine kinase

scFv: Single chain variable fragment

SRD: Significant residual disease

STAT3: Signal transducer and activator of transcription 3

TAA: Tumor-associated antigen

TAM: Tumor-associated macrophage

TAP: Transporter associated with antigen processing

TCGA: The Cancer Genome Atlas

T_{cm}: T central memory

T_{em}: T effector memory

TGFβ: Transforming growth factor β

T_H: T helper

TIL: Tumor-infiltrating lymphocyte

TMA: Tissue microarray

TMZ: Temozolomide

TNF: Tumor necrosis factor

TP53: Tumor protein 53

T_{reg}: T regulatory

TRAIL: TNF-related apoptosis-inducing ligand

TSA: Tumor-specific antigen

TTFs: Tumor treating fields

VEGF: Vascular endothelial growth factor

WASP: Wiskott-Aldrich syndrome protein

WHO: World Health Organization

ZAP-70: Zeta-chain-associated protein kinase 70

CHAPTER 1: General Introduction

1.1 Glioblastoma multiforme in the clinic

Glioblastoma multiforme (GBM) is an astrocyte-derived, high grade tumor that represents more than 60% of all adult tumors of the brain and 14% all primary CNS tumors[1,2]. Classified as a Grade IV glioma by the World Health Organization (WHO), GBM represents a relatively low fraction of all cancer diagnoses (10 cases per 100,000 globally), but it incurs a heavy cost to quality of life and is associated with a dismal survival (14-15 months median survival and 26.5% 2-year survival)[3,4]. Regrettably, this survival profile has plateaued for the past decade despite advances in the understanding of its pathophysiology, including the disrupted molecular pathways, pathological and molecular classification, and immune landscape, as well as development of targeted and immune-based therapeutic modalities, spanning small molecules, biologics, cell-based therapies, vaccines, and oncolytic viruses.

Most GBM cases arise *de novo* but around 10% are secondary, arising from diffuse astrocytoma or anaplastic astrocytoma. Primary GBM is seen in older adults at a mean age of 62 with predilection to males. It typically is located supratentorially and has extensive neovascularization and necrosis, partly due to elevated VEGF levels[5,6]. The primary identified risk factors thus far are history of ionizing radiation exposure from childhood brain cancer and leukemia treatment and genetic syndromes such as Li-Fraumeni syndrome, Lynch syndrome, and constitutional mismatch repair-deficiency syndrome. There is not an established link between GBM and electromagnetic

radiation, cell phone use, or head trauma[1,7]. Secondary GBM arises in a younger population at a mean age of ~45 with no gender preference, but with tendency to develop in the frontal lobe and have only limited necrosis[5,6]. While focal neurological signs depend on the tumor location, headache and seizures are the most common presenting symptoms and typically progress from days to weeks[7]. Increased intracranial pressure, mass effect, and edema can accompany relatively large tumors. Moreover, venous thromboembolisms, gastrointestinal disturbances, and mood disorders are commonly seen[8].

Current first line treatment for GBM consists of maximal resection (when applicable), chemoradiotherapy, and maintenance chemotherapy with or without tumor-treating fields (TTFs)[9]. Surgery is typically not curative because of the early infiltrative behavior of GBM, with residual tumor quickly reemerging[10]. Dexamethasone is typically used perioperatively to control cerebral edema and neurological side effects associated with radiotherapy[11]. However, corticosteroid use leads to many side effects of its own such as gastric bleeding, osteoporosis, opportunistic infections, and myopathy[8]. Furthermore, several recent lines of evidence have shown that corticosteroid use is associated with poorer survival, possibly through enhancing tumor cell radio-resistance[11,12]. In 2005, a Phase III trial of 573 patients across 85 centers led by Stupp and colleagues demonstrated that the use of radiotherapy concurrently with temozolomide (TMZ) followed by adjuvant TMZ improves median survival from 12.1 months to 14.6 months and 2-year survival from 10.4% to 26.5%, compared with radiotherapy alone[4]. This therapeutic approach (“The Stupp Regimen”) was one of two

recent major advancements in GBM therapy and became standard-of-care alongside surgical resection.

The other major therapeutic advancement was the use of TTFs, which are low-intensity, alternating electric fields applied to patients' brains via ceramic transducer arrays attached to the patients' bare scalp[9]. These fields have been shown to alter tubulin orientation during metaphase and cytokinesis, thereby disrupting sister chromatid segregation and mitosis. A randomized Phase III trial in recurrent GBM comparing TTFs alone to chemotherapy alone demonstrated equivalence with regards to median survival (6.6 months vs. 6.0 months), 1-year survival (20% vs. 20%), and PFS (21.4% vs. 15.1%)[13]. However, patients on TTFs had significantly fewer adverse events relative to the chemotherapy arm (6% vs. 16%), and quality-of-life measure such as cognitive functioning, emotional functioning, role functioning, and symptoms like loss of appetite, constipation, diarrhea, fatigue, nausea and vomiting, and pain, all favored TTFs over chemotherapy alone. This study led to the approval of TTFs by the FDA for recurrent GBM and paved way for a randomized, multicenter Phase III trial for new GBM diagnoses treated with TTFs concomitantly with maintenance TMZ versus maintenance TMZ alone (standard-of-care)[14]. An interim analysis of the trial showed that TTFs plus TMZ improved median progression-free survival (7.1 months vs. 4.0 months), median overall survival (20.5 months vs. 15.6 months), and 2-year survival (43% vs. 29%), leading to the approval of TTFs alongside TMZ for first-line therapy. There was no increased incidence of systemic side effects or seizures in the group receiving both TTFs and TMZ, but mild to moderate skin irritation at the scalp contact

site with the device is very common (seen in 43% of patients) and can be easily managed.

There is no standard therapy for recurrent GBM. Typically, the recurrent tumor characteristics (e.g. focal vs. diffuse, mass effect) and patient's treatment history determine the most appropriate approach, which consists of one or more of the following: surgical resection, TMZ, nitrosoureas, bevacizumab (humanized anti-VEGF monoclonal antibody), or clinical trial enrollment. Bevacizumab was rationally developed from the observation of high vascularity and VEGF expression in GBM, and that systemic inhibition of VEGF improves survival in preclinical rodent models[15,16]. It was granted accelerated approval by the FDA based on multiple Phase II trials demonstrating improved PFS, but not overall survival, in recurrent GBM patients administered bevacizumab with irinotecan[17,18]. The BELOB Phase II trial of bevacizumab monotherapy versus lomustine monotherapy or a bevacizumab-lomustine combination demonstrated an improvement in overall survival at 9 months, leading to the Phase III EORTC 26101 trial[19]. EORTC 26101 concluded the combination of bevacizumab plus lomustine improves PFS (4.2 months vs. 1.5 months) but not overall survival (9.1 months vs. 8.6 months) relative to lomustine alone, which was later supported by meta-analysis of clinical trials by Song and colleagues[20,21]. Nevertheless, the study confirmed previous observations that the addition of bevacizumab has anti-vasogenic edema properties that allows patients on dexamethasone for cerebral edema to reduce the dexamethasone dose[17,18]. These results led to the full approval of bevacizumab for recurrent GBM by the FDA in 2017. The persistent lack of overall survival benefit despite improved PFS associated with bevacizumab treatment has been

explained by several studies. Several groups have used orthotopic murine models to show that angiogenesis inhibition in fact promotes tumor progression, invasiveness, and metastasis through induction of hypoxia[15,22]. *In vitro* studies by Du *et al.* demonstrated in a Boyden Chamber invasion assay with mouse GBM cell lines that ectopic expression of VEGF or addition of recombinant VEGF reduces invasion[23]. Pieo and colleagues demonstrated that while anti-VEGFR via the inhibitor sunitinib reduces tumor vascularity to a greater extent than buvacizumab in murine xenograft model, it correspondingly induces greater hypoxia, and does not confer survival benefit, unlike bevacizumab. Furthermore, both bevacizumab and sunitinib promote mesenchymal changes such as increased smooth muscle actin and vimentin, as well as increased stem cells markers like nestin and Sox2[24]. Overall, while bevacizumab may initially slow tumor progression by normalizing tumor vasculature, medication-induced hypoxia drives cellular adaptations by tumor cells that promote tumor progression and aggressiveness, negating any overall survival benefit.

1.2 Molecular heterogeneity of GBM

GBM prognosis is poor across the board and the disease is invariably fatal. Nevertheless, recent molecular characterization of GBM unveiled two important prognostic factors: (1) O^6-methylguanine-methyltranseferase (MGMT) promoter methylation, and (2) isocitrate dehydrogenase 1 and 2 (IDH1/2) mutations[25,26]. MGMT repairs alkylated adducts, particularly at the O^6 position of guanine. Thus, the reduced expression of MGMT in GBM tumors with methylated MGMT promoter is believed to sensitize tumor cells to the alkylating effects of TMZ. Interestingly, part of the negative effect of corticosteroids on survival is believed to be due to their induction of MGMT

expression as well as stabilization of MGMT through upregulation of N-myc downstream regulated gene 1 (NDRG1). In fact, one study found *MGMT* promoter methylation was not predictive of TMZ response in patients treated with corticosteroids[27,28].

IDH1/2 enzymes produce NADPH from NADP+ by oxidative decarboxylation of isocitrate to α-ketoglutarate (α-KG). The mutations seen in GBM are exclusively missense mutations in an arginine residue in the active site: R132 in IDH1, with R132H seen in as high as 88% of cases, and correspondingly R172 in IDH2[29]. *IDH1/2*-mutated tumors are most often seen in secondary GBM and are a positive prognostic factor, while *IDH1/2* is rarely mutated in primary GBM[26,30]. In a cohort of 136 patients, Yan and colleagues found that patients with *IDH*-mutant GBM had a median overall survival of 31 months and that of *IDH*-wildtype GBM patients was only 15 months[29]. Exceptions to this pattern are believed to be due mis-classification of primary as secondary and vice versa. Primary GBM with mutant *IDH* may actually arise from undiagnosed secondary GBM as evidenced by the significant younger age of diagnosis and genetic similarities to secondary GBM as opposed to primary GBM[31,32]. On the other hand, secondary GBM with mutant *IDH* typically arise from grade II glioma while those with wildtype *IDH* usually arise from grade III glioma, raising the possibility that primary GBMs were misdiagnosed as grade III gliomas[32]. These mutations lead to reduced NADPH production, thereby reducing the tumor cells antioxidant supply and could account for the survival benefit[29,33]. Some lines of evidence suggest that mutant IDH exerts a dominant negative effect on wildtype IDH in IDH1-mutant GBM cells, thereby reducing wildtype IDH catalytic activity and NADPH levels[34]. However, coprecipitation studies comparing mutant IDH1 versus mutant IDH2 do not show binding of mutant IDH2 to the

wildtype allele[35]. Alternatively, or additionally, mutant IDH1 and IDH2 have been demonstrated to drive elevated 2-hydroxyglutarate (2-HG) levels, an oncometabolite produced by mutant IDH1/2 from α-KG that competitively inhibits α-KG-dependent enzymes[25,35].

Other genetic alterations seem to co-occur with the *IDH* mutational status. GBM tumors with wildtype *IDH* usually harbor *EGFR* and MDM2 overexpression or gain-of-function mutation (i.e. *EGFRvIII*), *PTEN* loss, *CDKN2A* deletion, and activating *TERT* promoter mutation, while those with mutant *IDH* co-occur with *MGMT* promoter methylation, loss-of-function mutations in *TP53* and *ATRX*, and *PDGFA* or *PDGFRa* overexpression. Generally speaking, receptor tyrosine kinase (RTK) (e.g. *EGFR, PDGF/R*) deregulation, phosphatidylinositol-3- OH kinase (PI3K) pathway activation, and *p53* and retinoblastoma (*Rb*) pathway disruptions were recognized to be the characteristic genetic alterations in GBM[32,36]. The alterations affect cell cycle control, DNA repair, survival, cell metabolism, differentiation, and angiogenesis. Importantly, the dichotomy between *IDH*-wildtype and *IDH*-mutant GBM tumors likely represents distinct gliomagenesis pathways. In fact, in 2016 the WHO updated its glioma classification guidelines to include both pathological and genetic profiles, as opposed to pathology alone, with the genetic profile taking precedence over the pathological one[6]. In this update, the “Glioblastoma” classification has been broken down into “Glioblastoma, IDH-wildtype”, “Glioblastoma, IDH-mutant”, and “Glioblastoma, NOS (not otherwise specified)”, with the IDH-wildtype category including three subclassification of rare GBM tumors: giant cell glioblastoma, gliosarcoma, and epithelioid glioblastoma.

Phillips and colleagues were the first to classify GBM based on gene expression in 2006 using microarrays, yielding the proneural, proliferative, and mesenchymal subtypes, based on tissue similarities. Each subtype correlated with genetic, genomic, histological, and clinical characteristics[37]. Their hypothesis that the mesenchymal subtype arises from the other subtypes was supported six years later by Li et al. in an extensive intra-tumoral aneuploidy analysis[38]. In 2010, Verhaak *et al.* used The Cancer Genome Atlas (TCGA) analysis of GBM to refine the classification proposed by Phillips *et al.* into: classical, mesenchymal, neural, and proneural[39]. The genetic signatures are as follows: (1) Classical: *EGFR* amplification or *EGFRvIII*, chromosome 10 loss, absence of *TP53* loss, loss of *CDKN2A* that is mutually exclusive with loss of RB pathway components, and overexpression of *NES*, Notch pathway, and Sonic hedgehog pathway genes. Notably, this subtype was the only one in which MGMT promoter methylation predicted TMZ response[36]. (2) Mesenchymal: *NF1* loss, expression of mesenchymal and astrocytic markers such as *CHI3L1*, *MET*, *CD44*, and *MERTK*, and overexpression of genes in the TNF super family and NF-κB pathways. (3) Proneural: *PDGFRA* overexpression or, in an almost mutually exclusive pattern, *IDH1* mutations. *TP53* loss, overexpression of oligodendrocytic and proneural development genes, and PI3K pathway mutations are also especially common in this subtype. Consistent with previous description of IDH-mutant GBM, the proneural subtype is associated with a diagnosis of secondary GBM and younger age of diagnosis. (4) Neural: expression of neuron markers like *NEFL*, *GABRA1*, and *SYT1*. Among the shared genomic alterations, chromosome 7 amplification and chromosome 10 deletions are almost invariably found in all subtypes except the proneural subtype where these

genomic events are seen at frequencies as low as 46% and 69%, respectively. While deletions at 9p21.3 harboring the *CDKN2A*/*CDKN2B* locus are commonly seen in all subtypes (in at least 56% of samples tested by Verhaak *et al.*), the classical subtype is particularly enriched for these deletions (95% of samples). The classical subtype also lacked *TP53* mutations (0% of samples) whereas at least 21% of samples in each of the other subtypes have *TP53* mutations. One group identified two clusters of cancer stem cells in GBM that correlated with the proneural and mesenchymal subtypes[40].

Arguably one of the most important conclusions of this study is that these subtypes were sustained in patient-derived murine xenograft models but immortalized GBM cell lines were enriched only for the mesenchymal subtype gene signature[39]. The lack of subtype recapitulation in immortalized cell lines has important implications in pre-clinical GBM studies. It establishes a concrete translational aspect to patient-derived xenograft models that can help personalize a drug in development to patients with certain GBM subtypes. For example, Verhaak and colleagues showed that GBM subtype correlate with better response to radiochemotherapy or prolonged chemotherapy regimens in, somewhat surprisingly, all but the proneural subtype.

Several other groups proposed different subtype classification such as those derived from nuclear morphology, genotype, and outcomes data[41], from gene expression and copy number aberrations[42], or from epigenetic markers[43]. The Noushmehr classification is of particular importance because it further refines the Verhaak molecular classifications. Noushmehr and colleagues used TCGA data to identify a subset of GBM tumors with a CpG island methylator phenotype (CIMP) similar to that previously characterized in colorectal cancer, which they have designated as

glioma CIMP (G-CIMP). Nearly all G-CIMP tumors (87.5%) in their data set belong to the proneural molecular subtype and the G-CIMP+ proneural samples are particularly associated with clinical and molecular features of secondary GBM, even relative to the G-CIMP- proneural samples. This study also showed that lower grade gliomas are enriched for G-CIMP, further supporting the association of G-CIMP with secondary GBM, and that G-CIMP status is retained in GBM from diagnosis to progression. Despite the differences in GBM classification among the different groups, all classifications converge on a GBM subtype associated with younger age at diagnosis, secondary GBM clinical diagnosis, longer survival, *IDH* mutations, and lack of chromosome 7 amplification and chromosome 10 loss. The discovery of these molecular subtypes has been in a boon to the field by expanding the understanding of the underlying GBM biology and allowing for informative subgroup analysis in preclinical and clinical trials. For example, Sandmann and colleagues retrospectively analyzed the results of the Phase III clinical trial for newly diagnosed GBM of bevacizumab plus chemoradiotherapy versus chemoradiotherapy only by the Phillips molecular GBM classification, showing that bevacizumab addition confers a significant PFS benefit in both the mesenchymal and proneural subtypes, but an overall survival benefit only in the proneural tumors[44]. Yet the discovery of GBM subtypes has made the task of finding effective treatment for GBM much more daunting as it elucidated the high level of heterogeneity in the disease. Subsequent work further complicated this goal by revealing that a single tumor mass may harbor foci of varying subtypes, and that the level of intratumoral heterogeneity negatively correlates with survival[45–47].

1.3 Targeted therapies for GBM

The importance of tumor molecular heterogeneity for treating GBM is further highlighted by the failure of molecularly targeted therapies to produce significant survival benefits. The molecular characterization of GBM stimulated the rational development or repurposing of small molecules, vaccines, monoclonal antibodies, and antibody-drug conjugates (ADCs) targeting recurrent genetic abnormalities seen in GBM, yet none of these approaches have produced a compelling case for clinical approval[48,49]. Studies have suggested that treatment failure can be at least partially explained by molecular heterogeneity leading to target-negative recurrence or recurrence with mutations in the targeted pathway leading to drug insensitivity. While some overall and progression-free survival benefit may be seen in a subset of patients in clinical trials of targeted therapies, durable response is rarely seen, if at all. There are other obstacles to efficacy, such as poor blood-brain barrier (BBB) penetration, variation in sensitivity of the drug target to inhibition, metabolism by hepatic cytochrome P450 enzymes induced by anticonvulsants or other medications, and intolerable toxicities, but the proven intra- and intertumoral molecular heterogeneity cannot be overlooked. Anticonvulsants that induce hepatic cytochrome P450 enzymes also have been shown to reduce the efficacy of some of these inhibitors, and some clinical trials stratified patients according to the patients' anticonvulsant regimen.

Not only is EGFR often amplified or harbors gain-of-function alterations in GBM, overactive EGFR signaling has been implicated in many aspects of GBM tumorigenesis, igniting the testing of EGFR-directed therapeutic approaches[50]. Gefitinib, erlotinib, and lapatinib are first-generation reversible small molecule inhibitors of EGFR and HER2, while afatinib, dacomitinib, and neratinib are second-generation irreversible inhibitors[48].

First-generation inhibitors did not show efficacy as monotherapy for recurrent GBM or in addition to radiation or chemoradiation for newly diagnosed GBM in Phase II trials due to poor brain penetration (erlotinib, lapatinib)[51,52] and/or insufficient inhibition of the EGFR pathway that may be due to redundant activating mutations in the pathway or low sensitivity to the inhibitors (gefitinib, erlotinib, lapatinib), or alternatively due to paucity of patients harboring EGFR alterations[48,53,54]. However, the second-generation, pan-EGFR inhibitor dacomitinib also echoed limited benefit in recurrent GBM as monotherapy in a patient population enriched for EGFR-altered tumors[55]. Vivanco *et al.* provided compelling evidence to show that while the EGFR kinase domain-binding inhibitor erlotinib effectively reduces EGFR activation in the lung cancer kinase domain-mutated EGFR variant, it has little effect on the extracellular domain-mutated EGFRvIII found in GBM; lapatinib, which binds the EGFR inactive conformation, is more effective against the GBM variant[54]. The role of molecular heterogeneity in limiting response to EGFR inhibitors can be appreciated through several studies. Analysis of tumors from small groups of patients treated with either gefitinib or erlotinib as monotherapy suggested that co-expression of EGFR and PTEN strongly correlated with clinical response, but only 24-26% of patients had clinical response[56]. Another group demonstrated that coactivation of multiple RTKs can maintain PI3K signaling when one RTK is inhibited (i.e. by erlotinib or the MET inhibitor SU11274), but co-inhibition by both inhibitors successfully abrogates PI3K pathway signaling[57]. Not only does PTEN need to be intact, but also other RTKs are likely needed to be inactivated to achieve clinical response to EGFR inhibitors.

Appreciation of this molecular complexity of GBM led to studies of drugs targeting multiple RTKs or inhibitors of downstream signaling (PI3K/mTOR inhibitors) with or without RTK inhibitors or other approved therapies, albeit without promising results. Dasatinib targets the kinases PDGFR, c-Kit, Src, and EphA2, which are implicated in GBM pathogenesis and drug resistance and was tested in a Phase II single-arm study of patients with first recurrence of GBM following the Stupp regimen and confirmed overexpression or overactivity of at least two of the drug targets[58]. There was no radiological response observed and median overall and progression-free survival measures were poor (7.9 months and 1.7 months, respectively). Another drug, imatinib, targets the two GBM-relevant tyrosine kinases PDGFR and c-Kit, and has been demonstrated to be efficacious in preclinical GBM models[59]. A Phase II study of imatinib in 20 GBM patients demonstrated that, despite presence of the drug in tumor tissue, tumor proliferation rate did not change and biochemical response was variable and seen in only 4 of 11 evaluable patients; the median overall survival of the patients was merely 6.2 months. Notably, there was no selection of patients based on PDGFR and/or c-Kit characterization. The use of the mTOR inhibitors everolimus and temirolus as single-agents or in combination with standard therapy has not shown efficacy[49]. Even the pan-PI3K inhibitor buparlisib, which has been shown to cross the BBB and reduce PI3K pathway activation in some patients, has not shown efficacy as monotherapy in recurrent GBM patients enriched for PI3K pathway activation[60,61]. Many of the clinical trials with inhibitors of RTKs or downstream PI3K pathway inhibitors have also not seen a correlation between response and target expression or target pathway inactivation[48,49]. The hurdles to clinical response with these approaches are multifold.

Not only there is molecular heterogeneity in the target protein and its downstream pathway, but the drug also has to pass the BBB and achieve sufficient concentration throughout the tumor to not only inactivate the PI3K pathway and stop tumor growth, but also to lead to tumor cell death. With such variegated and complex tumor biology in GBM, it is not surprising that small molecule inhibitors failed to reach the market.

Approaches with fewer barriers to exert antitumor effects, like immune-based approached, have been explored. An EGFRvIII-specific peptide vaccine called rindopepimut was developed by Celldex Therapeutic and entered clinical trials[62]. This approach relies on the presence of EGFRvIII to be effective, rather than on the activity level of the EGFR downstream pathway as in the case of EGFR and other RTK/PI3K/mTOR inhibitors. While this overcomes the barrier of molecular heterogeneity in the PI3K pathway, it still has to overcome the heterogeneity of EGFRvIII expression within a tumor, as well as any immune escape mechanisms employed by GBM[63]. Unlike many RTK/PI3K pathway inhibitors, rindopepimut has reached Phase III clinical trials (ACT IV) but addition of monthly ridopepimut plus GM-CSF intradermal injections to TMZ had no improvement in median overall survival relative to control injection plus TMZ (20.1 months vs. 20.0 months, respectively) in the group with minimal residual disease (MRD)[62]. The study observed a potential 2-year overall survival benefit in the group with significant residual disease (SRD) (30% vs. 19%, $p = 0.029$) but the statistical significance was eliminated when the patients were classified by the study investigators as opposed to by the central review. The investigators speculate that this benefit could stem from the higher burden of EGFRvIII-expressing tumor cells in patients with SRD as opposed to MRD. Both in this study and in earlier clinical trials of

rindopepimut, tumor escape was confirmed by loss of EGFRvIII expression at recurrence, suggesting that tumor molecular heterogeneity plays a role in treatment failure[62,64]. Moreover, another group was able to detect inflammatory cytokine release from EGFRvIII-activated TILs from patient tumor samples, indicating that the host is able to mount a native immune response to EGFRvIII but it is insufficient to control the tumor. The same mechanisms that prevent control of the tumor by the native immune response may contribute to the failure of rindopepimut[63,65]. These data are encouraging however as they demonstrate that immune cells from the periphery can mobilize to the tumor site in the brain and exert antitumor efficacy, which can be exploited in the development of further immunotherapies.

AbbVie's depatuxizumab mafodotin (depatux-m), an ADC made of the EGFR-specific monoclonal antibody depatuxizumab and the microtubule disruptor monomethyl auristatin F (mafodotin) is another promising immune-based, EGFR-directed investigational therapeutic[66]. Mafodotin is designed to be released only when the depatuxizumab-EGFR/EGFRvIII complex is internalized by the tumors. Moreover, depatuxizumab is selective only for overexpressed EGFR and EGFRvIII, but not wildtype EGFR expressed at physiological levels. This clever recognition of EGFR targets a specific epitope that is exposed only in overexpressed EGFR or EGFRvIII. Depatux-m showed mixed results in Phase III trials, with lack of benefit in newly diagnosed GBM (Intellance 1 trial) but encouraging results in recurrent GBM (Intellance 2 trial). In Intellance 1, patients with EGFR-amplified newly diagnosed GBM were given either standard therapy (the Stupp regimen) with placebo or standard therapy with depatux-m. Interim analysis of 639 patients showed the drug failed to confer any

survival benefit and the trial was stopped (NCT02573324). It is possible that, as in the case of rindopepimut, reduced altered EGFR burden post-resection limited the efficacy of depatux-m in Intellance 1. The choice of conjugated drug can also have impact on efficacy, as one study showed that pyrrolobenzodiazepine-conjugated anti-B7-H3 ADC was able to eliminate tumor cells and vasculature, while monomethyl auristatin E (MMAE)-conjugation only eliminated the tumor cells[67]. In Intellance 2, EGFR-amplified patients with recurrent GBM were either given depatux-m, depatux-m and TMZ, or TMZ or lomustine[68]. The depatux-m plus TMZ, when compared to the TMZ/lomustine group, showed a hazard ratio of 0.68 (95% CI 0.48-0.95, p = 0.024) and 1-year overall survival of 40% vs. 28%. The average depatux-m concentration in the patients, but not the extent of EGFR amplification predicted survival. Just as in the case of rindopepimut, depatux-m relies primarily on the presence of tumor-specific molecular alterations (i.e. EGFR amplification / EGFRvIII) for efficacy, but not on their activity. However, immunosuppressive mechanisms are not expected to play a role in treatment failure here since it is a cell-free therapy.

1.4 Antitumor immunity

TCGA shed light on the immunological heterogeneity of GBM, which has important implications for immunotherapies[69]. The complexity of antitumor immunity and the tumor immune microenvironment have only relatively recently begun to be appreciated, but the concept of antitumor immunity was recognized as early as 50 years ago[70]. Early experiments demonstrating that inbred mice can be immunized against syngeneic tumor transplants gave rise to the idea that tumors harbored tumor-specific antigens and that immunosurveillance – the elimination of tumor cells by the immune

system – is a characteristic of the immune system[71]. The first strong piece of evidence demonstrating the role of lymphocytes in suppressing both carcinogen-induced and spontaneous tumors came about when Shankaran *et al.* showed that recombination activating gene 2 (RAG-2) deficient mice had other incidence of such tumors[72]. Moreover, Shankaran *et al.* showed that tumors transplanted from RAG-2 deficient mice onto isogenic wildtype mice were rejected while those transplanted from wildtype to RAG-$2^{-/-}$ mice were not, suggesting that the immune system influences the immunogenicity of tumors. Work by many groups has led to a three-phase "Cancer Immunoediting" theory to be adopted to explain the role of the immune system in eliminating and sculpting tumors in both mice and humans: (Phase 1) Elimination: the immune system eliminates precancerous cells, (Phase 2) Equilibrium: tumor clones that evaded immune destruction are kept in check by lymphocytes and IFNγ that put selective pressure on the tumor to evolve clones that are resistant to immune influence, and (Phase 3) Escape: immunologically-resistant clones grow, form an immunosuppressive microenvironment, and eventually become clinically apparent[73].

T cells play a central role in adaptive antitumor immunity. Generally speaking, CD8+ cytotoxic T cells (CTLs) have a direct effector role in destruction of cancer cells and CD4+ helper T cells (T_H cells), especially T_H1 cells, help in orchestrating the antitumor response by releasing cytokines like IFNγ and TNFα and chemokines like MCP-1 (CCL2)[74,75]. However, the existence of immune-suppressing regulatory CD8+ T cells in autoimmunity and CD4+ CTLs in cancer has been documented[76,77]. T cell activation by tumor cells requires three signals: (1) Engagement of the CD3-bound T cell receptor (TCR) with MHC-bound tumor peptide antigen, (2) co-stimulation

classically by engagement of the target cell's CD80 (B7-1) or CD86 (B7-2) with the T cell's CD28, and (3) stimulation by cytokines in the microenvironment. At the immune synapse, CD8 allows CTLs to bind to MHC Class I molecules found on every nucleated cell while CD4 allows T_H cells to bind MHC Class II molecules, which are found on professional antigen presenting cells (pAPCs) like dendritic cells (DCs) and macrophages. Signal 1 leads to the phosphorylation of immunoreceptor tyrosine-based activation motifs (ITAMs) found on the cytoplasmic tails of CD3 subunits, which leads to recruitment of several signaling molecules involved in T cell activation, such as lymphocyte-specific protein tyrosine kinase (Lck), zeta-chain-associated protein kinase 70 (ZAP-70), non-catalytic region of tyrosine kinase (Nck), and Wiskott-Aldrich syndrome protein (WASP)[78]. Signal 2 further enhances T cell activation and promotes processes such as T cell proliferation, differentiation, survival, and cytokine production[79]. The diversity of co-stimulatory molecules is vast and their specific roles and interactions are beginning to be understood. For example, CD28 has been shown to directly associate with PI3K to activate the PI3K/AKT/mTOR pathway, leading to T cell proliferation and survival, and to associate with Lck to promote IL-2 production. 4-1BB is a distinct co-stimulatory molecule that can have overlapping functions as CD28 such as enhanced proliferation via AKT activation, survival, and memory response formation. Differences between the two co-stimulatory molecules have also been clarified, such as the bias of 4-1BB to induce CD8+ CTL but not CD4+ T cell expansion and the superior role of CD28 on naïve T cell priming[79,80]. The cytokines provided in signal 3 are important for the differentiation of CD4+ T helper cells into subsets of effectors cells (e.g. T_H1, T_H2, T_H17, T_{reg}) which will then release more cytokines that will

determine the type of immune response that will be mounted[81]. In the case of antigen-activated CD8+ T cells, the presence of cytokines provided in signal 3, specifically IL-12 and IFNα/β, determine if the T cell will respond to the antigen, proliferate, and differentiate, or if the cells will tolerate the antigen and be deleted or anergic. Upon activation, CD8+ CTLs may eliminate a target cell through several mechanisms. For one, CD8+ CTLs can release intracellular granules containing perforin and granzyme B, where the perforin polymerizes in the target cell membrane and creates pores for granzyme B to diffuse across and induce apoptosis through caspase cleavage[82,83]. The effector cytokine IFNγ can also be released by CTLs, thereby inhibiting tumor proliferation and angiogenesis[84]. The cell-surface molecules FasL and TRAIL can induce apoptosis by binding Fas and TRAIL-R, respectively, on tumor cells, leading to recruitment of the death-inducing signaling complex (DISC) that activates caspase and causing cell death[85].

The same mechanism used by CD8+ CTLs to eliminate non-malignant cells such as virus-infected cells is used to eliminate malignant cells. In the case of virus-infected cells, viral peptides generated from proteasomal degradation are translocated into the endoplasmic reticulum (ER) through transporter associated with antigen processing (TAP), where they bind MHC Class I molecules[86]. MHC Class I molecules are composed of an integral membrane heavy chain whose extracellular region is made of three α domains with α_1 and α_2 forming the peptide-binding groove, and the β2 microglobulin protein. Through the ER and Golgi apparatus, the MHC-peptide complex is transported to the cell surface, where it can be recognized by CD8+ CTLs. Professional APCs such as DCs play a crucial role in priming T cells to eliminate

tumors[87]. As pAPCs, DCs express MHC Class II, through which they present endosome-internalized, protease-cleaved tumor peptide antigens to CD4+ T cells and lead to their activation through the three-signal mechanism described above. It is the cytokines from DCs that are major dictators of the differentiation lineage of the T_H cells, primarily promoting T_H1 differentiation by releasing IL-12 and IFNγ. On the other hand, in the process of cross-presentation, endosome-internalized tumor antigens are presented on MHC Class I molecules through one of two hypothesized pathways: (1) Vacuolar pathway: The antigen is internalized into and degraded by lysosomal proteases such as Cathepsin S, and then loaded onto MHC Class I molecules inside the lysosome (as opposed to in the ER) that are then translocated to the cell membrane. (2) Endosome-to-cytosol pathway: The internalized antigen is transported into the cytosol where it is degraded by the proteasome and then either returned to the endosome to be loaded onto MHC Class I molecules or it goes through the “traditional” TAP-dependent MHC I loading in the ER.

One important difference between detection of virus-infected cells and transformed cells is that viral antigens are inherently foreign to the immune system and are thus more likely to incite an immune response. On the other hand, since transformed cells are derived from the host, they inherently contain only proteins the exist in the host. Thus, what drives the detection and elimination of these cells are neoantigens generated from mutations or presentation of native peptides that have not been tolerated for during T cell thymic maturation[88]. Tumor-specific antigens (TSAs) are those that are unique to the tumor cells, such as mutation-derived neoantigens, oncogenic virus-derived peptides, cancer-germline antigens, or alternatively transcribed

gene products; EGFRvIII is an example of a TSA in GBM because it is not found in normal cells. Tumor-associated antigens (TAAs) are those that are also found in some normal cells but can be characteristic (e.g. overexpressed) of the tumor, such as the amplified EGFR in GBM. TSAs and TAAs are essentially a manifestation of the underlying tumor biology; they are a product of the mutation-driven tumor evolution and progression, even if the antigens themselves are not mutated. Thus, TSAs and TAAs either contribute directly to tumor survival as in the case of amplified EGFR or EGFRvIII, or they are a byproduct of genetic alterations. Either way, in congruence with the cancer immunoediting theory, the TSAs and TAAs arise from antitumor immunity-mediated sculpting of cancer, and therefore play some role in determining the tumor immune milieu.

The diversity of known tumor-infiltrating immune cells has grown dramatically over the years, with some contributing to the tumor's immunosuppressive microenvironment, while others reflect the host's antitumor immunity. TILs may not only include CD8+ T cells but also CD4+ T cells, T_{reg} cells, $\gamma\delta$ T cells, NK cells, NKT cells, B cells, and B_{reg} cells[89–92]. Intratumoral myeloid cells, such as myeloid-derived suppressor cells (MDSCs), M1 proinflammatory macrophages, M2 immunosuppressive macrophages, neutrophils, and dendritic cells are also extensively involved in tumor progression and antitumor immunity[93–96]. It has been shown that even stromal cells such as cancer-associated fibroblasts may secrete cytokines and chemokines, thereby contributing to the tumor immune microenvironment[97,98]. In fact, the tumor immune infiltrate is a dynamic landscape that changes with tumor progression[99]. Ratios of different infiltrating immune cells, typically an antitumor effector cell and

immunosuppressive cell, have been shown to be strong predictors of outcomes in multiple malignancies, such as the CD8+/T_{reg} ratio in epithelial ovarian cancer survival[100], T cell/MDSC ratio in non-muscle invasive bladder cancer recurrence[101], and neutrophil/lymphocyte ratio in hepatocellular carcinoma survival[102]. It is the balance between antitumor immunity and tumor-associated immunosuppression that determines disease progression and outcomes.

1.5 GBM immune microenvironment and heterogeneity

Immunosuppressive mechanisms employed by tumors are diverse and shared across cancer types, and in some cases redundant. Work from multiple groups over the years have shown that GBM utilizes both cell-based and molecular mechanisms to evade host immunity. Immunosuppressive T_{reg} cells can originate either in the thymus during T cell development (natural, nT_{reg}) or in the periphery when CD4+ T cells become tolerant of peripheral antigens (induced, iT_{reg}). The presence of T_{reg} cells in human GBM and murine GBM models has been documented by multiple groups[103–105]. Wainwright and colleagues demonstrated that intratumoral T_{reg} cells in GBM are primarily thymus-derived, as indicated by high level of co-localization of the nT_{reg}-specific transcription factor Helios and the T_{reg}-specific transcription factor FoxP3 in both human and mouse GBM samples[105]. Both types of T_{reg} cells exert their immunosuppressive actions through the production of immunosuppressive cytokines like TGFβ and IL-10, starving of nearby T cells of IL-2 by overexpressing IL-Rα (CD25) that is part of the IL-2 receptor, and depriving T cells of co-stimulation by expressing CTLA-4 which outcompetes CD28 for CD80 and CD86 on APCs.

Tumor-associated macrophages (TAMs) are traditionally seen as having one of two opposing phenotypes: The M1 proinflammatory phenotype that participates in antitumor immunity through antigen presentation and inflammatory cytokine secretion and the M2 immunosuppressive phenotype that contributes to the tumor's immune evasion, tissue invasion, and metastasis[106]. Both peripheral M2 macrophages and resident macrophages (microglia) have been shown to play a role in tumor progression and high M2 TAM levels are associated with poor clinical prognosis in GBM[103,106,107]. One group showed that GBM TAMs lack expression of the T cell co-stimulatory molecules CD80, CD86, and CD40, even though they expressed MHC Class II molecules[103]. Komohara and colleagues showed that direct contact between M2 TAMs and GBM tumor cells promotes tumor progression through the STAT3-activating properties of TAMs, which has also been implicated in driving cancer stem cells (CSCs) in GBM[106,107]. This may be more so true for tumors of the mesenchymal subtype, as it has been shown that the mesenchymal phenotype is heavily driven by STAT3 in GBM[108]. Conversely, a study by Wu *et al.* demonstrated that GBM CSCs secrete soluble CSF-1, TGF-β1, and MIC-1 which recruit macrophages and microglia and polarize them to the M2 phenotype[109]. This was further supported by priming macrophages with GBM CSC-conditioned media, causing them to polarize to the M2 phenotype, halt phagocytosis, secrete IL-10 and TGF-β1, and impair T cell proliferation. Another possible interplay between GBM cells and the TAMs is seen in EGFR-altered GBM[110]. Analysis of M1 and M2 markers in orthotopic murine xenografts of U-87 MG tumors expressing either EGFR, EGFRvIII, or both shows that xenografts expressing both EGFR and EGFRvIII have higher levels of both M1 and M2 macrophages relative

to xenograft expressing either EGFR or EGFRvIII. Yet, it is likely that the M2-polarizing microenvironment of GBM can shift the ratio to favor M2 TAMs. Vlaicu's group primed primary human monocytes and macrophages to supernatant of multiple breast cancer cell lines and demonstrated the release of EGFR ligands[111]. While this may not necessarily apply to GBM, it is possible that a positive feedback between GBM EGFR signaling-dependent macrophage recruitment and polarization and macrophage secretion of EGFR ligands propagates an immunosuppressive tumor microenvironment.

MDSCs are immunosuppressive CD11b+Gr-1+ cells that arise in conditions of chronic inflammation like cancer and can be classified into either polymorphonuclear (PMN-MDSCs) or monocytic (M-MDSCs), with most cancers having a PMN-MDSC-predominant population[112]. PMN-MDSCs induce antigen tolerance by nitrating TCR leading to decreased sensitivity to stimulation by peptide-MHC complexes, nitrating T cell chemoattractants, and inhibiting the binding of tumor peptide antigens to MHC Class I molecules using the free radical peroxynitrite (PNT). M-MDSCs use both antigen-dependent and antigen-independent mechanisms of immunosuppression and are considered more immunosuppressive than PMN-MDSCs. In addition to producing PNT, they express high levels of iNOS which produced nitric oxide (NO) and of ARG1 which depletes L-arginine for T cells to use[113]. GBM patients show elevated levels of both PMN-MDSC and M-MDSC in the circulation, but tumor tissue from these patients shows a predominant PMN-MDSC population[114].

Several cell surface molecules play a role in immunosuppression in GBM. FasL is expressed by both human and rat GBM tumor cells and plays a role in suppressing T cell-mediated antitumor immunity, as seen by the lack of survival benefit in FasL

knockdown tumor in athymic rats relative to immunocompetent rats[115]. The NK cell inhibitory molecule lectin-like transcript-1 (LLT1) has been shown to be expressed by GBM *in vitro* and *in vivo*, and even upregulated by TGFβ, a known immunosuppressive cytokine in the GBM microenvironment[116]. The upregulation of the checkpoint molecule PD-L1 in GBM correlates with the molecular subtype[117]. Analysis by Berghoff *et al.* of GBM specimen and TCGA data revealed that low PD-L1 expression was typical of the proneural subtype and G-CIMP+ tumors, while elevated PD-L1 expression was associated with the mesenchymal subtype. Overall, most newly diagnosed (88.0%) and recurrent (72.2%) cases exhibited some level of PD-L1 expression, yet there was no difference in PD-L1 expression or TIL density between newly diagnosed and recurrent GBM specimen, and no association between PD-L1 expression or TIL density with outcomes. Interestingly, while PTEN loss has been shown to increase PD-L1 expression[118], there was no correlation between PD-L1 expression and PTEN status in this study.

B7-H3 is a member of the B7 superfamily of immunomodulatory molecules with a controversial function. Its expression has been documented in both DCs and T cells and evidence for both a T cell co-stimulating and inhibiting function have been demonstrated with the immunosuppressing evidence dominating[119–121]. Recently, B7-H3 gained attention due to its ubiquitous expression in many different types of cancers, including GBM, as well as tumor-associated vasculature[122,123]. TCGA analysis of B7-H3 expression revealed it is elevated in IDH-wildtype GBM, especially in the mesenchymal subtype, and that it is correlated with a worst prognosis[123]. Moreover, *In vitro* studies suggest that B7-H3 promotes CSC-like phenotype and invasiveness in GBM cell

lines[123,124]. Importantly, Lemke and colleagues demonstrated that B7-H3 contributes to tumor progression in GBM in part by suppressing NK cell-mediate tumor lysis, and that B7-H3 expression in GBM is inversely correlated with CD8+ cell infiltration[124]. Thus, B7-H3 likely also contributes to GBM's immunosuppressive environment.

As reviewed above, tumorigenesis and the tumor immune microenvironment are intricate, heterogeneous, interrelated, and dynamic aspects of GBM. Doucette's group sought to clarify the relationship between GBM molecular subtypes and the immune microenvironment by characterizing the immune signature of each subtype from TCGA data[69]. Interestingly, they found that the mesenchymal subtype was enriched for both immune activators and immune inhibitory genes relative to the classical and more so relative to the proneural subtypes. The immunosuppressive cytokines IL-10, IL-23, and TGFβ were present to a greater extent in the mesenchymal subtype relative to the proneural subtype. On the other hand, indicators of CD8+ CTL activators were overexpressed (MICB, IL-7, and IL-15). Also, while the apoptosis-inducing Fas and PD-L1 were enriched in this subtype, so was the T cell co-stimulating OX40L. CCR2 and its ligand MCP-1, which are involved in monocyte chemoattraction were both highly enriched in the mesenchymal type (2.5- and 3.7-fold relative to the proneural subtype), implying a central role of TAMs. Indeed, galectin-1, which has been shown to correlate with the M2 macrophage marker CD163 and inhibit M1 macrophages, galectin-3, which is secreted by M2 macrophages, and STAT3, which promotes CSCs to recruit TAMs and is itself activated by TAMs, are all overexpressed in the mesenchymal subtype. Furthermore, the role of MDSCs is highlighted by the enrichment for arginase. TNFRSF14, also known as herpesvirus entry mediator (HVEM), is 2.3-fold

overexpressed in the mesenchymal relative to the proneural subtype. This can have important implications in oncolytic virus therapy for GBM. Herpes simplex virus (HSV)-based oncolytic therapies are being developed for glioblastoma[125,126], and preferential expression of HVEM on mesenchymal GBM could influence the efficacy of such approach on this subtype. Doucette *et al.* noted that NK cell-related genes were not enriched in any particular molecule GBM subtype, except for CD244, which activates NK cells, being enriched in the proneural subtype. They also tested for expression of known GBM antigens across the different subtypes to evaluate whether enrichment of these antigens in the mesenchymal subtype accounts for the increased immune cell concentration. While the no subtype preferentially expresses all GBM antigens relative to all the other subtypes, each subtype has a bias to a different profile of GBM antigens. Relative to the proneural samples, the mesenchymal samples overexpressed EGFR, Her2, Epha2, Sart-2, and gp100, but were deprived of Survivin, B-cyclin, and Sart-1. The neural subtype has the least diversity in overexpressed GBM antigens, with only EGFR seen in 54% of samples and Survivin in 20% of samples; the rest of the antigen are seen at frequencies of 16% or less. The predilection of EGFR alterations in the classical subtype was confirmed by the presence of EGFR antigens in 80% of the samples. Thus, the immune classification of GBM by Doucette's group illuminated primarily on differences between the most dissimilar subtypes: mesenchymal versus proneural. As concluded in the manuscript, it suggests that the mesenchymal subtype may be the most immunogenic subtype and thus most amenable to immunotherapies.

1.6 Chimeric antigen receptor T cells in cancer

In light of the numerous immunosuppressive mechanisms in GBM and the molecular classification, and still the desperate need for therapies that will change the survival landscape of GBM patients, chimeric antigen receptor (CAR) T cells have been developed for GBM. CARs are synthetic molecules composed of an extracellular single chain variable fragment (scFv) derived from a monoclonal antibody linked by a hinge region to a transmembrane domain that is attach to an intracellular T cell-activating molecule such as the CD3ζ chain with or without one or more co-stimulatory domains (e.g. CD28, 4-1BB)[127]. In essence, CAR T cells are T cells with the antigen specificity of B cells. Engagement of the scFv to the target antigen induces T cell activation, proliferation, survival, and differentiation via phosphorylation of ITAM domains on the CD3ζ chain, leading to recruitment of downstream signaling molecules like Lck, ZAP-70, and others. First generation CARs lack a co-stimulatory molecule in tandem with the CD3ζ chain, while second generation CARs have one co-stimulatory domain, and third generation have two. Fourth generation CARs have two co-stimulatory domains plus another element to enhance CAR T efficacy or safety[128]. While CAR technology has taken on various forms divergent from the classical structure, such as bi-specific CARs[129], inhibitor CARs[130], CARs with synthetic transcription factors[131], and even CAR circuits that reduce on-target, off-tumor effects[132], this discussion will focus on traditional CARs because there is the greatest amount of clinical data available for this type in GBM.

CAR Ts are inherently resistant to several immunosuppressive mechanisms employed by many tumors, including GBM. Because CAR Ts recognize antigens in their native state, as opposed to an MHC-bound peptide antigen, they are not affected by

mutations or downregulations of genes in the antigen processing and presentation pathway, such as *TAP1*, *TAP2*, *BM2*, and *HLA* genes[133]. Moreover, the co-stimulatory domains of CAR Ts obviates the need for co-stimulatory signal from the target tumor cells, which often downregulate such molecules and can induce the downregulation of these molecules on pAPCs[134,135]. Just like depatux-m, CAR T efficacy depends on the presence of their target but not on modification of its biological activities, as in the case of RTK inhibitors. Since the antigen-recognition domain of CAR Ts is antibody-derived, the CAR can in fact recognize non-protein targets. Nevertheless, CAR Ts also have their limitations. Their target antigens are limited to only cell surface molecules, which can be downregulated or mutated[136]. Also, since they are a cell-based therapy, they are amenable to influence of the tumor immune microenvironment, including immunosuppressive cells, cytokines, and cell surface molecules[137]. Persistence is a major issue for CAR T cells, as both the immunogenicity of the CAR ectodomain can induce an anti-CAR immune response[138] and the differentiation of activated CAR Ts may produce short- or long-living effector and memory cells depending on the co-stimulation signal[139].

The process of producing CAR T cells in expensive and time-intensive. Autologous T cells are isolated from the patient's blood, expanded *in vitro* in antigen-independent manner, and transduced with either a lentivirus or retrovirus containing the CAR construct before further expansion[140]. Lymphodepletion of the patients with chemotherapy prior to CAR T cell adoptive transfer has been shown to improve expansion, efficacy, and persistence[141]. Multiple groups have been working on "off-the-shelf" universal CAR T cells to allow for scalability of CAR T therapy[128]. Moreover, the

choice of T cell population from which CAR T cells are generate can have large impact on the efficacy and safety of the treatment *in vivo* by having different antitumor, persistence, trafficking, and activation profiles[127]. Memory T cells, specifically central (T_{cm}) and effector (T_{em}) memory, have shown superiority to effector T cells due to their greater proliferative potential and persistence[142]. The *in vitro* culture conditions of CAR T cells, including the cytokines and stimulation mode employed, can have a profound effect on their *in vivo* efficacy. Gargett *et al.* demonstrated that in their GD2-specific third generation CAR T cells, the combination of stimulation with via both CD3 and CD28 and expansion with both IL-7 and IL-15 yielded the optimal balance of CAR T cell expansion, effector function, and stem/memory phenotype[143].

Two severe adverse effects have been recurrently documented in clinical trials of CAR T therapies: cytokine release syndrome (CRS) and neurotoxicity. CRS occurs due to massive CAR T cell activation leading to a large release of inflammatory cytokines such as IL-6, TNFα, and IFNγ[127,144]. Its presentation varies with severity but it is common to see hypotension, coagulopathy, neurological disturbances such as delirium, seizures, headache, and aphasia, cardiac dysfunction, rash, and constitutional symptoms like fever, fatigue, myalgias, and arthralgias. Management of CRS consists of the anti-IL-6 antibody tocilizumab with or without corticosteroids. Neurotoxicity occurs often with CRS but can also arise separately[145]. The symptoms are similar to those seen in CRS: encephalopathy, delirium, tremor, seizures, and aphasia. Elevations in inflammatory cytokines like IL-6, IL-2, and GM-CSF and T cells in the cerebrospinal fluid and brain tissue have been observed in non-human primate models. While some cases of CRS and neurotoxicity can be self-limiting, others can be fatal[144,146]. Other

documented toxicities associated with CAR T cell therapy are on-target but off-tumor effects that are dependent on the target antigen, such as B cell aplasia in the context of CD19-specific CAR T cells[140]. These toxicities need to be managed on a case-by-case basis by can be mitigated by choosing a target antigen with low expression on normal cells.

There are currently only two FDA-approved CAR T therapies, tisagenlecleucel (Kymriah) by Novartis and axicabtagene ciloleucel (Yescarta) by Kite Pharma, both of which target CD19 and are indicated for various hematological malignancies: (relapsed/refractory) diffuse large B cell lymphoma, pediatric acute lymphoblastic leukemia, primary mediastinal B cell lymphoma, and high grade B cell lymphoma. Both approved therapies are second generation CARs with tisagenlecleucel having the 4-1BB co-stimulatory molecule and axicabtagene ciloleucel having the CD28 domain[147]. Much of the success of CD19-directed CAR T cells can be attributed to the choice of antigen and nature of the malignancy. CD19 is highly expressed almost invariably on most B cell leukemias and non-Hodgkin's lymphoma, and otherwise expressed only on normal B cells[140]. While B cell aplasia is a common side effect in CD19-specific CAR T treatment, it can be easily managed by immunoglobulin replenishment. The hematological nature of the indicated malignancies is an advantage of CAR T therapy, which are typically delivered intravenously into patients. Thus, the presence of both the CAR T cells and tumor cells in the vasculature obviates the need for enhancing the trafficking of the CAR T cells into a specific tissue site, as in the case of solid tumors.

CAR T therapy has reached only limited success in solid tumors thus far. Molecular heterogeneity in solid tumors has hindered the efficacy of many different

antigen-redirected CAR T cells. While evidence of antitumor efficacy and trafficking to the tumor is indeed observed[148,149] tumor immune escape prevents CAR T cells from achieving durable clinical benefit[150]. Of note, recurrence with CD19-negative tumor has also been documented in B cell hematological malignancies treated with CD19-directed CAR T cells, such as B-ALL[151]. In contrast to leukemias and lymphomas, CAR T cells given for solid tumors need to traffic to the tumor site, but tumor cells and tumor-associated endothelium modify chemokine and chemokine receptor expression to limit T cell trafficking[152]. The immunosuppressive microenvironment established by solid tumors, as well as variable areas of perfusion, hypoxia, and nutrient availability, also need to be overcome for CAR T cells to show efficacy[147,152].

1.7 CAR T therapy for GBM

CAR T therapies that target EGFRvIII, HER2, and IL13Rα2 in GBM have been tested in clinical trials with variable results, but invariable tumor progression leading to patient death[150,153,154]. Preclinical studies of CSPG4- and EphA2-directed CAR T cells have also shown promise in preclinical models[155–157]. The clinical evidence of antitumor activity against GBM by CAR T cells is encouraging as it demonstrates that efficacy can be reached despite the challenges mentioned above. Nonetheless, the lack of durable benefit and recurrence of antigen-negative tumor point to the challenge molecular heterogeneity holds for GBM. To that end, there are various preclinical studies aiming to use CAR T cells to target multiple GBM-associated antigens, such as the HER2-IL13α2-EphA2 trivalent CAR[158] or the CAR targeting both EGFRvIII and GBM-specific EGFR using one scFv[159]. Wang *et al.* claim that another way to optimize CAR T therapy for GBM is to selectively modify CD4+ T cells to express IL13α2-specific CAR, as they

showed CD4+ CAR T cells have superior antitumor efficacy and persistence in GBM preclinical models and are in fact impaired by the presence of CD8+ CAR T cells[160].

There is a unique opportunity with GBM to surmount the problem of CAR T trafficking. Given that part of the standard treatment is surgical resection, it is be possible to deliver the CAR T cells directly to the tumor site or through an intracranial reservoir perioperatively, as was done in clinical trials of IL13α2-specific CAR T cells, to enrich the cells in the tumor tissue[153,161]. Yet, clinical studies from intravenously-delivered CAR T demonstrate that they can cross the BBB and reach tumor in the brain[150,154]. One particularly interesting case of a patient with recurrent multifocal GBM was reported by Brown *et al.*[161]. The patient received multiple infusions of IL13α2-redirected CAR T cells both into the resected tumor cavity and into the ventricles over 220 days, leading to regression of all brain and spinal lesions that lasted for 7.5 months. Even more encouraging, all adverse effects observed were only grade 1 or 2. The safety, efficacy, and advantageous delivery opportunities of CAR T cells demonstrated in these clinical studies bode for a promising future of CAR T therapy for GBM. Molecular heterogeneity still remains one of the largest obstacles in this malignancy, and the need for identifying CAR targets that are more homogenously expressed within and across tumors remains urgent.

1.8 Summary

GBM is one of the most devastating malignancies, not only is the patient's quality-of-life greatly affected by the tumor and its mass and neurological effects, but most patient die within 1-2 years of diagnosis. Our understanding of the molecular basis of GBM along with its microenvironment has stemmed the development of

numerous therapies without much progress in survival benefit. These studies have stressed the role of intra- and intertumoral heterogeneity in treatment failure. CAR T cell immunotherapy is a promising therapeutic approach for GBM due to its selective antitumor activity, safety profile, resistance to multiple tumor immunosuppressive mechanisms, and advantageous delivery methods. However, a CAR target antigen that sufficiently controls tumor progression in light of GBM's molecular heterogeneity has not been identified yet. My preclinical studies of B7-H3-specific CAR T cells provide encouraging evidence to suggest B7-H3 has the potential to be an ideal CAR antigen for GBM treatment.

CHAPTER 2: B7-H3-redirected chimeric antigen receptor T cells target glioblastoma and neurospheres[1]

2.1 Overview

The dismal survival of GBM patients urgently calls for the development of new treatments. CAR T cells are an attractive strategy, but preclinical and clinical studies in GBM have shown that heterogeneous expression of the antigens targeted so far causes tumor escape, highlighting the need for the identification of new targets. We explored if B7-H3 is a valuable target for CAR-T cells in GBM through characterization of B7-H3 expression in publicly available data and GBM specimen, CSC-containing neurospheres (NS), and cell lines; and through comparison of two second-generation, B7-H3-specific CAR constructs in *in vitro*, tissue xenograft, and murine xenograft models of both GBM cell lines and GBM-NS. We have demonstrated that B7-H3 is highly expressed across GBM subtypes, and that B7-H3-redirected CAR-T cells can effectively control tumor growth in all models tested. Therefore, B7-H3 represents a promising target in GBM.

[1] This chapter has been submitted to *EBioMedicine* in 2019: Nehama D, Di Ianni N, Musio S, Du H, Patané M, Pollo B, Finocchiaro G, Park JJH, Dunn DE, Edwards DS, Damrauer JS, Hudson H, Floyd SR, Ferrone S, Savoldo B, Pellegatta S, Dotti G. "B7-H3-redirected chimeric antigen receptor T cells target glioblastoma and neurospheres". Experiments, data collection, data analysis and interpretation, and manuscript writing were done primarily by me. Of note, I did not perform any of the experiments involving primary human GBM samples and GBM neurospheres.

2.2 Introduction

GBM is an aggressive, malignant brain tumor with abysmal survivorship[62]. Treatment typically consists of surgical resection followed by radiation therapy. The addition of temozolomide increased the median survival (from 12.1 to 14.6 months) and 2-year survival rate (from 10.4% to 26.5%)[4]. Observations of extensive vascular proliferation in GBM led to the use of the VEGF inhibiting monoclonal antibody (bevacizumab) that also improved the progression free survival and quality-of-life of the patients, but not overall survival[162].

The systematic molecular assessment of GBM indicates that RTK genes and the PI3K, p53 and Rb pathways are dysregulated[36]. The identification of these genetic events led to the development of various targeted therapies, such as EGFR-targeting drugs (afatinib, erlotinib, ADCs), and PI3K inhibitors (buparlisib). However, GBM is characterized by great molecular heterogeneity, and different areas within a single tumor can fall under different classification[47], which partially explains the modest improvement of clinical outcome with targeted therapies[49].

CAR-T cells are T lymphocytes genetically modified to express a synthetic receptor that produces activation of the T cell machinery and co-stimulatory pathways upon ligation with a cell surface antigen expressed by tumor cells[127]. CD19-targeting CAR-T cells are FDA-approved for the treatment of refractory/relapsed B-cell malignancies[151,163]. The activity of CAR-T cells in hematologic malignancies stimulated the development of similar strategies in solid tumors including GBM. CAR-T cells targeting EGFRvIII, HER2, and IL-13Rα2 have shown a favorable safety profile and some clinical benefits in patients with GBM[150,154,161]. However, tumors recur with evidence of immune escape due, at least in part, to antigen loss. New promising

antigens such as EphA2 and CSPG4 characterized by high expression in GBM have been explored in preclinical studies[155,156], but tumor heterogeneity remains a concern highlighting the need for the continuous identification of new targets.

Here we report that B7-H3, a member of the B7-family[164], is highly expressed in over 70% of GBM specimens, and invariably expressed by patient-derived GBM-NS, while it is not detectable in the normal brain. The expression of B7-H3 in GBM-NS is particularly relevant since these cells not only recapitulate the molecular properties of the primary GBM when expanded *in vitro* or engrafted in immunodeficient mice[165,166], but are also considered to be enriched in putative CSCs[167]. B7-H3-specific CAR-T cells showed antitumor activity both *in vitro* and in xenograft murine models with either GBM cell lines or GBM-NS, indicating that targeting B7-H3 allows the elimination of both differentiated tumor cells and CSCs.

2.3 Results

2.3.1 B7-H3 is expressed in GBM specimens

To assess the expression profile of B7-H3 in GBM, we first evaluated the B7-H3 mRNA expression (Gene name: *CD276*) in the TCGA dataset. GBM showed relatively high B7-H3 expression, with about 77% of samples lying above the mean B7-H3 expression of all TCGA tumors (Fig. S2.1). Importantly, B7-H3 was found expressed at similarly elevated levels in primary and recurrent GBM relative to normal brain tissue (Fig. 2.1A). In addition, B7-H3 mRNA levels also had the smallest variance as compared to the other molecules such as *CSPG4*, *EPHA2*, *ERBB2*, and *IL13RA2* that are targeted with CAR-T cells (Fig. 2.1A). Since mRNA levels do not necessarily directly predict protein expression, we evaluated the B7-H3 protein expression by

immunohistochemistry in a cohort of 46 GBM specimens previously studied for the expression of CSPG4[156]. We observed a diffuse positivity of B7-H3 expression, with 76% (35/46) of the specimens displaying a strong immunoreactivity for B7-H3, and 22% (10/46) showing detectable but low expression (Fig. 2.1B-E, Table 2.1). B7-H3 was not detected in one specimen. B7-H3 expression was mainly located into the plasma membrane of tumor cells. Among GBM with high B7-H3 expression, 41% were assigned to the classical subtype, 34% to the mesenchymal subtype and 25% to the proneural subtype (Table 2.1). Of note, tumor cells recruited in the vicinity of blood vessels, as well as adjacent normal-infiltrating tumor cells, were intensely positive for B7-H3 (Fig. S2.2). To further validate these results, we also stained commercially available human tissue microarrays containing GBM specimens (n = 32) and normal brain (n = 69) spanning various central nervous system structures as well as the optic nerve. All GBM samples overexpressed B7-H3 relatively to normal brain samples (Fig. 2.1F, G).

2.3.2 B7-H3-redirected CAR-T cells target human GBM cell lines *in vitro* and *in vivo*

We generated B7-H3-redirected CAR (B7-H3.CAR) T cells encoding either CD28 or 4-1BB endodomains (B7-H3.CD28 and B7-H3.41BB, respectively)[168], and CD19-redirected CAR (CD19.CD28) T cells[169] as control through retroviral transduction of activated T cells from healthy donors (Fig. 2.2A, B). CAR-T cells were then tested for antitumor activity against the U-87 MG and U-138 MG human GBM tumor cell lines, which express B7-H3, while the B7-H3-negative HL-60 leukemia cell line served as a negative control (Fig. 2.2C). B7-H3.CAR-T cells showed complete or near complete

elimination of U-87 MG and U-138 MG cells five days after seeding at 1:5 and 1:10 E:T ratios, as measured by the number of tumor cells remaining, with no statistically significant difference between B7-H3.CD28 and B7-H3.41BB CAR-T cells. There was no evidence of killing in wells seeded with CD19.CD28 CAR-T cells or control non-transduced T cells (cT) and in wells seeded with HL-60 cells (Fig. 2.2D, E). We measured cytokine release by CAR-T cells in the coculture supernatant after 24 hours and CAR-T cell proliferation in response to antigen stimulation. The effector cytokines IFNγ and IL-2 were detected in the supernatant only when B7-H3.CAR-T cells were cocultured with U-87 MG or U-138 MG cells, with B7-H3.CD28 CAR-T cells showing higher cytokine release as compared to B7-H3.41BB CAR-T cells (Fig. 2.3A, B). To examine the proliferative capacity of B7-H3.CAR-T cells in response to antigen stimulation, we labeled the T cells with CFSE and cocultured them with U-87 MG, U-138 MG, or HL-60 cells at a 1:1 E:T ratio. After 5 days in coculture, B7-H3.CAR-T cells proliferated only in response to U-87 MG and U-138 MG cells, with no statistical difference seen between B7-H3.CD28 and B7-H3.41BB CAR-T cells. No proliferation was observed in CD19.CD28 CAR-T and cT cells (Fig. 2.3C, D).

The antitumor activity of B7-H3.CAR-T cells was then tested in a xenograft murine model. We first generated U-87 MG cells stably expressing *GFP-FFLuc* (U87-GFP-FFLuc) (Fig. S2.3). U87-GFP-FFLuc were then injected intracranially into the caudate nucleus of *nu/nu* mice. One week later, mice were treated intratumorally with CD19.CD28, B7-H3.CD28 or B7-H3.41BB CAR-T cells. Tumor growth was monitored by BLI (Fig. 2.4A). In each experiment, mice were assigned a treatment such that the pre-treatment tumor BLI distribution was comparable in each treatment group. Among

mice with initial tumor burden <1 x 10^8 p/sec/cm^2/sr total flux, sustained tumor regression was seen in 86% (6/7) and 100% (5/5) of those treated with B7-H3.CD28 CAR-T cells or B7-H3.41BB CAR-T cells, respectively (Fig. 2.4B, C). B7-H3.CAR-T cell treatment conferred a significant and prolonged survival benefit, with no significant difference between B7-H3.CD28 and B7-H3.41BB CAR-T cells (Fig. 2.4D). Post-mortem analyses of tumors harvested from mice treated with either CD19.CAR or B7-H3.CAR-T cells revealed retention of the B7-H3 expression in tumor cells (Fig. 2.4E) indicating that tumor recurrence is not caused by antigen loss. No treatment-related adverse effects were observed. We could not assess the effects of B7-H3.CAR-T cells in mice engrafted with U-138 MG cells because this tumor cell line had inconsistent engraftment, and when engrafted was characterized by very slow tumor growth with no morbidity even months after engraftment. To further prove that B7-H3.CAR-T cells can target tumor cells *in situ*, we developed a xenograft rat brain slice coculture model in which U87-GFP-FFLuc or GBM-NS-GFP cells are seeded onto rat brain slices and treated 1 day later with either CD19.CAR-T cells, B7-H3.CAR-T cells, or no cells (Fig. 2.4F, G). Cytokine quantification of supernatant 24 hours after CAR-T cell treatment reveals IFNγ and IL-2 release only in the presence of B7-H3.CAR-T cells, with B7-H3.CD28 CAR-T cells releasing more IFNγ and IL-2 in 2 out of 3 U87-GFP-FFLuc-seeded brain slices and more IL-2 in 2 out of 2 GBM-NS-GFP-seeded brain slices. Similar levels of IFNγ were released by B7-H3.CD28 and B7-H3.41BB CAR-T cells in all GBM-NS-GFP-seeded slices (Fig. 2.4H, I).

2.3.3 B7-H3-redirected CAR-T cells target human GBM-NS *in vitro* and *in vivo*

Since GBM established tumor cell lines do not fully recapitulate the molecular subtypes of human GBM and do not mimic human cancer stem cells, we sought to test B7-H3.CAR-T cells against patient-derived GBM-NS[170]. We measured the expression of B7-H3 in 20 GBM-NS representative of the most common GBM molecular subtypes. We found high expression levels of B7-H3 (ranging from 89% to 100% of cells) in all GBM-NS, independently of their molecular subtype (Fig. 2.5A, B, Table 2.1). We tested the antitumor activity of B7-H3.CAR-T cells against five representative GBM-NS. The killing ability of B7-H3.CAR-T cells was evaluated by flow cytometry in a coculture assay at different time points using 1:5 E:T ratio. B7-H3.CAR-T cells encoding CD28 showed prominent antitumor efficacy already at 24 hours as compared to those encoding 4-1BB. However, at 48 hours B7-H3.CD28 and B7-H3.41BB CAR-T cells equally eliminated GBM-NS from the culture (residual GBM-NS < 2%). In contrast, GBM-NS continued to grow in the presence of CD19.CD28 CAR-T cells (Fig. 2.5C). The T_H1 cytokine profile in the supernatant in response to GBM-NS revealed more IFNγ release by B7-H3.CAR-T cells encoding 4-1BB only in two out of the five GBM-NS tested. This result correlates with the upregulation of PD-L1 in GBM-NS upon exposure to IFNγ as we have previously reported[156] (Fig. 2.5D). However, B7-H3.CAR-T cells encoding CD28 released higher amount of IL-2, consistent with the *in vitro* studies with U-87 MG and U-138 MG cell lines (Fig. 2.5E).

To test *in vivo* the antitumor activity of B7-H3.CAR-T cells against GBM-NS, *nu/nu* mice were implanted with GBM-NS into the brain, and CAR-T cells or control T cells were injected intratumorally 15 days later (Fig. 2.5F). B7-H3.CAR-T cells encoding

either CD28 or 4-1BB equally controlled the tumor growth and prolonged the survival in 50% of the treated mice as compared to mice treated with control T cells (Fig. 2.5G). Morphological analyses performed on explanted brains showed high cellularity in control xenograft gliomas. On the contrary, in B7-H3.CAR-T cell-treated xenograft gliomas the architecture was disrupted by large damaged and necrotic areas (Fig. 2.5H, I).

2.4 Discussion

One of the greatest barriers to developing effective immune therapies for GBM is the heterogeneity of antigen expression within and across tumors, which highlights the need of the identification of novel targets. We report that B7-H3 is highly expressed in GBM and can be effectively targeted using B7-H3-specific CAR-T cells. Furthermore, B7-H3 expression is highly conserved in patient-derived GBM-NS supporting the potential of the proposed strategy to eradicate tumor cells with high tumor regenerative capacity.

Clinical trials of CAR-T cells in GBM patients have demonstrated tumor regression after either systemic or intracranial delivery routes[150,154,161]. Nonetheless, these trials also highlighted how tumor antigen escape due to the heterogeneous expression of the antigens hinders the durability of clinical responses. A bioactivity and safety study of IL13Rα2-targeted $CD8^+$ CAR-T cells by Brown *et al.* documented recurrence of IL13Rα2-negative tumors[153,161]. Similarly, O'Rourke and colleagues described recurrence of antigen-negative tumors in patients with GBM treated with EGFRvIII-directed CAR-T cells[150]. The identification of antigens that are invariably expressed by tumor cells, but not by the counterpart normal cells remains a high priority to target solid tumors, including GBM, with CAR-T cells. We have previously reported

that targeting CSPG4 in GBM partially addresses the issue, because CSPG4 is highly expressed in 67% of the GBM specimens we tested, and is also expressed in tumor-associated vessels, but not in normal cerebral vessels and normal brain[156]. Furthermore, we observed that CSPG4 expression can be induced by TNFα released by resident microglia, and potentially by TNFα secreted by CAR-T cells upon activation[156]. In this study, we report that B7-H3 is also highly expressed in 76% of GBM, but not in normal brain tissue, and that targeting B7-H3 via CAR-T cells promotes antitumor activity both *in vitro* and in xenograft models highlighting the clinical relevance of B7-H3 as a molecular target in GBM. However, as previously observed for CSPG4[156], a third of the GBM specimens analyzed show low expression of B7-H3, and this level of expression may be insufficient to promote effective killing by CAR-T cells as we have recently reported[168]. However, the data presented in this report demonstrate that B7-H3 is almost invariably expressed in patient-derived GBM-NS spanning all molecular GBM subtypes. Furthermore, GBM-NS are effectively targeted by B7-H3-redirected CAR-T cells both *in vitro* and *in vivo*. GBM-NS are generated from human GBM samples using the same growth factors employed for neural stem cells and are enriched in putative cancer stem cells[167]. Since several lines of evidence indicate that cancer stem cells have a critical role in causing tumor recurrence[166,171,172], effectively targeting these cells with B7-H3.CAR-T cells offers greater potential to control tumor recurrence even if some differentiated tumor cells may not be eliminated because they express B7-H3 at low levels.

Occurrence of cerebral edema and cytokine release syndrome has been attributed to CAR-T cells in hematologic malignancies[173]. Clinical studies of CAR-T cells

in GBM patients have shown a relatively favorable safety profile, with no dose-limiting toxicities seen for HER2- and EGFRvIII-redirected CAR-T cells[150,154], and manageable grade 3 events (headache, neurologic deficits) in patients treated with high dose anti-IL13Rα2 CAR-T cells intracranially[153,161]. The B7-H3.CAR we have developed shows cross-reactivity to murine B7-H3, yet in our experimental setting we did not observe macroscopic adverse effects in both xenograft and immunocompetent murine models[168]. Furthermore, in a clinical study in which the ^{131}I-conjugated B7-H3 Ab was administered to patients with metastatic neuroblastoma, no toxicity was encountered[174]. These data, as well as the lack of B7-H3 expression in the central nervous system, reported in this and our previous study[168], suggest that on-target but off-tumor toxicity may not occur in human subjects.

We observed only limited differences in the antitumor activity of B7-H3.CAR-T cells encoding either CD28 or 4-1BB costimulatory domains both *in vitro* and *in vivo*. As previously reported[175], we observed that CD28 co-stimulation provides faster antitumor effects as compared to 4-1BB co-stimulation, but this did not translate into enhanced antitumor activity in the experimental conditions we have used *in vitro* and *in vivo*. The intratumor delivery route of the CAR-T cells may confer immediate exposure of the CAR-T cells to tumor cells and overcome the difference in cytokine release we observed *in vitro* between CD28 and 4-1BB co-stimulation, leading to equivalent antitumor efficacy *in vivo*. Of note, nearly all the mice with large initial tumor burden failed treatment irrespective of the provided co-stimulation, highlighting the importance of additional studies aimed at enhancing the persistence of CAR-T cells within the tumor

environment to eradicate large tumors or the need of early detection of tumor recurrence and early treatment.

In conclusion, our study shows that B7-H3 is an attractive target in GBM since it is highly expressed in 76% of the GBM specimens tested and is invariable expressed in GBM-NS that contain cancer stem cells, while B7-H3 is not detectable in normal brain. B7-H3-redirected CAR-Ts control tumor growth and B7-H3 expression is retained at tumor recurrence indicating that strategies aimed at enhancing the CAR-T cell delivery and persistence within the tumor may further increase the efficacy profile of B7-H3-redirected CAR-T cells in GBM.

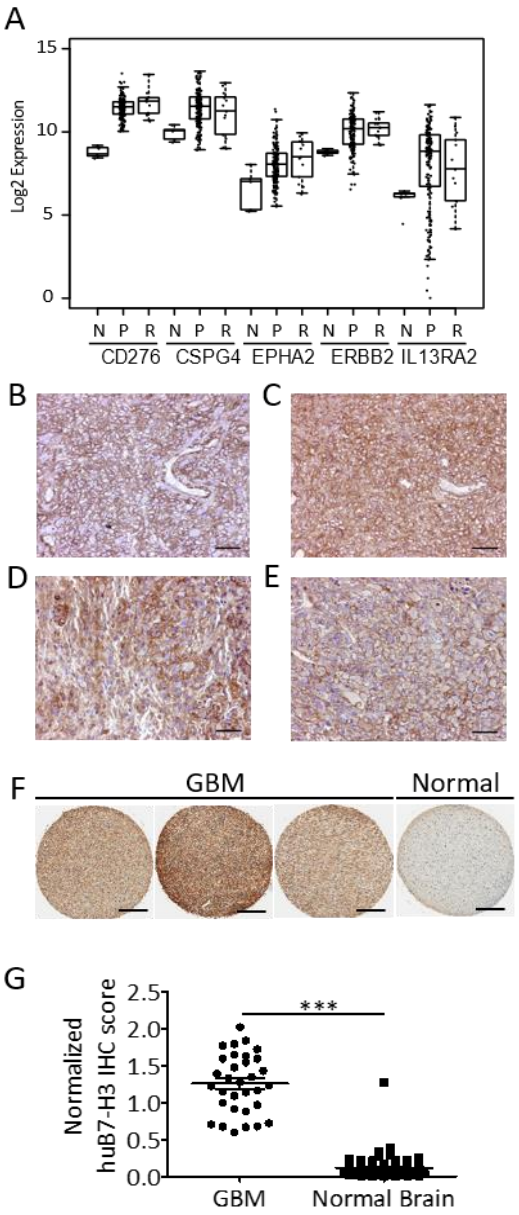

Figure 2.1 B7-H3 expression in GBM

(A) Normalized mRNA levels of *CD276* (B7-H3), *CSPG4*, *EPHA2*, *ERBB2*, and *IL13RA2* in adjacent normal ("N"), primary GBM ("P"), and recurrent GBM ("R") samples in TCGA. Each point represents a different TCGA sample. (B-E). Representative examples of B7-H3 immunostaining in classical (B), proneural (C), mesenchymal GBM (D), and a rare case of giant cell GBM (E). (F) Representative B7-H3 immunostaining of commercially available GBM tissue arrays and normal brain. (G) B7-H3 expression scores of the tissue microarrays of GBM (n = 32) and normal brain cores (n = 69) quantified via color deconvolution algorithm. Statistical analysis of difference in means was performed using two-tailed nonparametric Mann-Whitney U test (***$p<0.0001$). Scale bar B-E, 50 μm. Scale bar F, 400 μm.

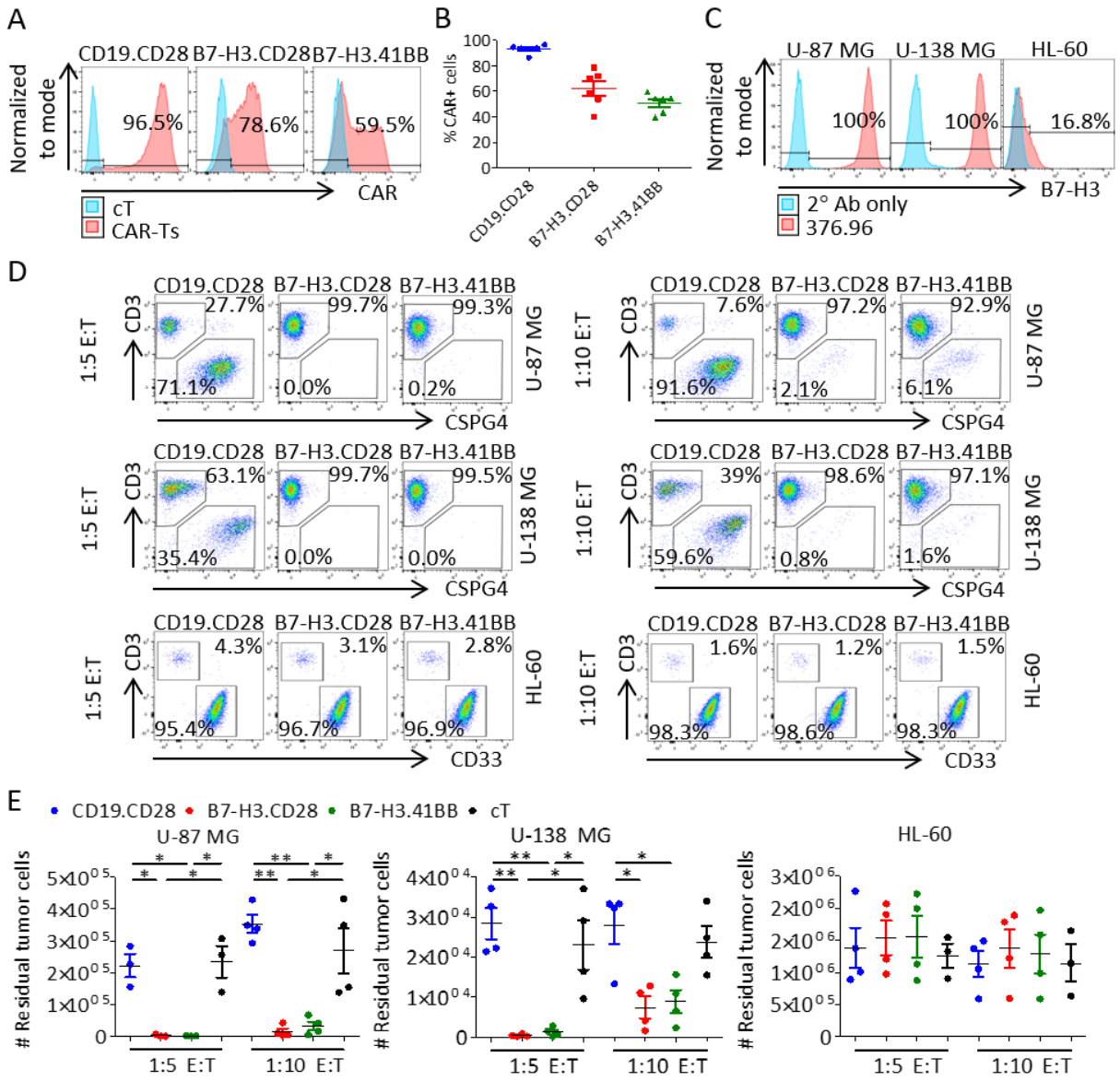

Figure 2.2 B7-H3.CAR-T cells target human GBM cell line *in vitro*

(A) Representative plots showing the CAR expression in CD19.CD28, B7-H3.CD28 and B7-H3.41BB CAR-T cells as assessed by flow cytometry and as compared to control T cells (cT). (B) Summary of CAR expression. Data represent mean ± SD (n = 6). (C) Expression of B7-H3 in U-87 MG, U-138 MG, and HL-60 cells stained with the 376.96 mAb and APC goat anti-mouse (GAM) and assessed by flow cytometry. (D) Representative flow cytometry plots of CAR-T cells ($CD3^+$) co-cultured with U-87 MG cells ($CSPG4^+$), U-138 MG cells ($CSPG4^+$), or HL-60 cells ($CD33^+$) at 1:5 or 1:10 effector-to-target (E:T) ratios for five days. (E) The number of remaining U-87 MG, U-138 MG, or HL-60 cells in 1:5 and 1:10 E:T coculture experiments in (D). Tumor cell numbers were calculated using counting beads. Data represent mean ± SD (n = 3 - 4). Difference in means was assessed through one-way ANOVA with Bonferroni's post-test correction (*p<0.05, **p<0.01).

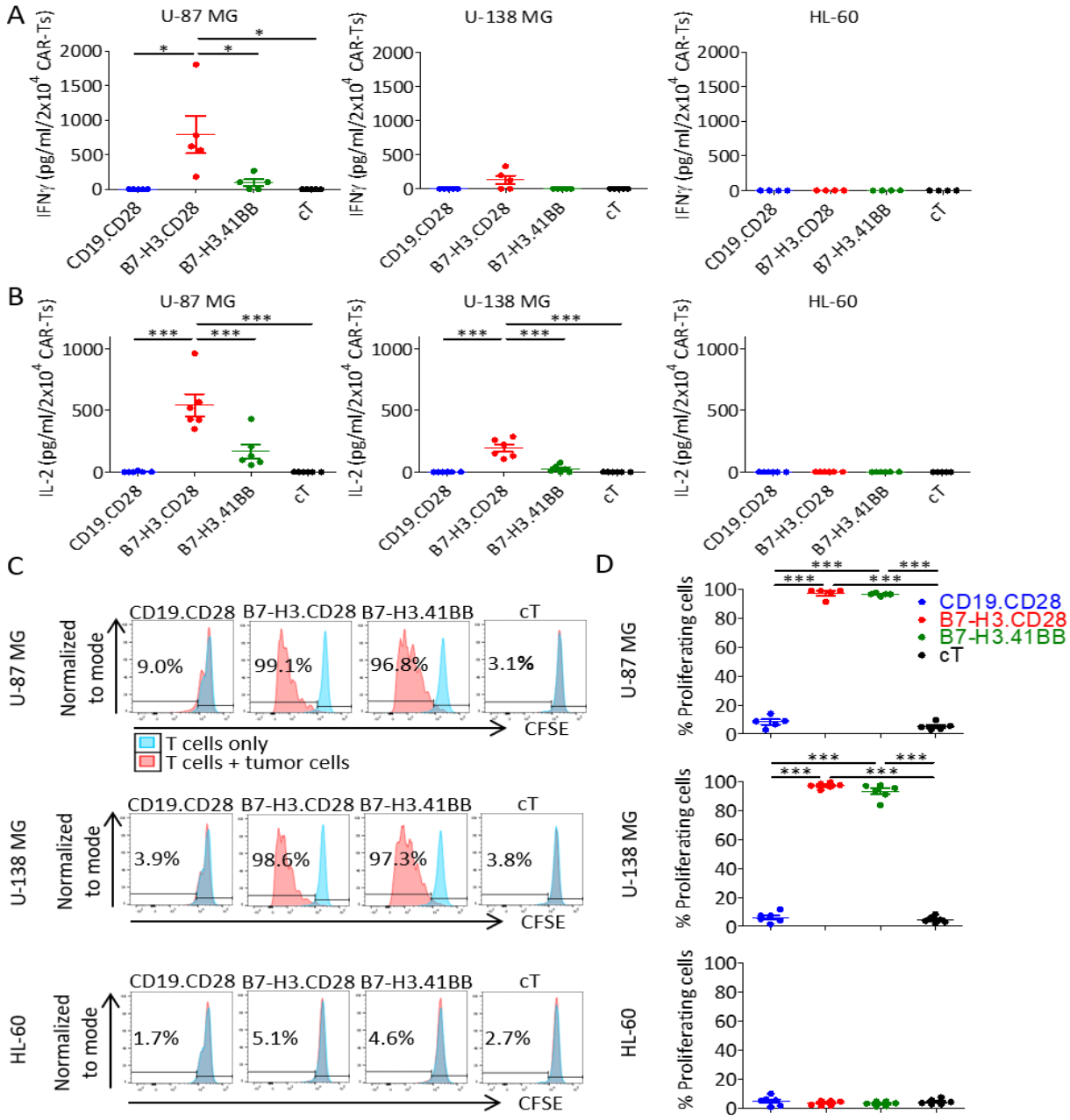

Figure 2.3 B7-H3.CAR-T cells release effector cytokines and proliferate in response to B7-H3$^+$ GBM cell lines

(A-B) Quantification of IFNγ (A) and IL-2 (B) by ELISA in the supernatant 24 hours after coculture of CAR-T cells or cTs with U-87 MG, U-138 MG, or HL-60 cells at 1:5 E:T ratio. Data represent mean ± SD (n = 5 - 6). Difference in means was assessed through one-way ANOVA with Bonferroni's post-test correction (*p<0.05, ***p<0.0001). (C) Representative CFSE dilution of CFSE-labeled CAR-T cells cocultured at a 1:1 E:T ratio with U-87 MG, U-138 MG, or HL-60 cells. (D) Summary of CFSE-dilution assays. Data represent mean ± SD (n = 5 - 6). Difference in means was assessed through one-way ANOVA with Bonferroni's post-test correction (***p<0.0001).

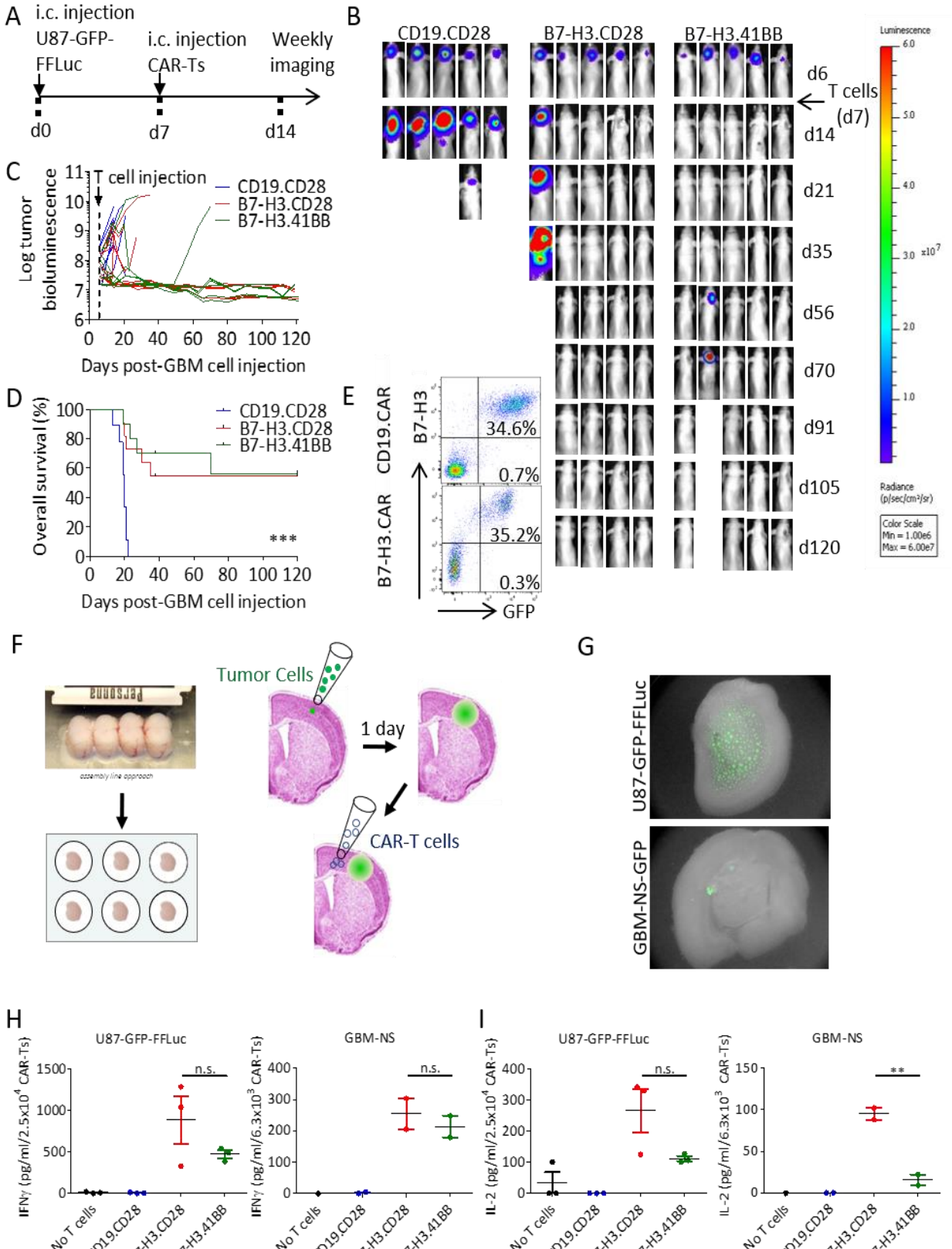
A
i.c. injection
U87-GFP-FFLuc
i.c. injection
CAR-Ts
Weekly imaging
d0
d7
d14
B
CD19.CD28
B7-H3.CD28
B7-H3.41BB
d6
T cells (d7)
d14
d21
d35
d56
d70
d91
d105
d120
Luminescence
Radiance (p/sec/cm²/sr)
Color Scale
Min = 1.00e6
Max = 6.00e7
C
T cell injection
CD19.CD28
B7-H3.CD28
B7-H3.41BB
Log tumor bioluminescence
Days post-GBM cell injection
D
CD19.CD28
B7-H3.CD28
B7-H3.41BB
Overall survival (%)
***
Days post-GBM cell injection
E
B7-H3
CD19.CAR
B7-H3.CAR
GFP
34.6%
0.7%
35.2%
0.3%
F
Tumor Cells
1 day
CAR-T cells
G
U87-GFP-FFLuc
GBM-NS-GFP
H
U87-GFP-FFLuc
GBM-NS
IFNγ (pg/ml/2.5x10⁴ CAR-Ts)
IFNγ (pg/ml/6.3x10³ CAR-Ts)
n.s.
No T cells
CD19.CD28
B7-H3.CD28
B7-H3.41BB
I
U87-GFP-FFLuc
GBM-NS
IL-2 (pg/ml/2.5x10⁴ CAR-Ts)
IL-2 (pg/ml/6.3x10³ CAR-Ts)
n.s.
**

Figure 2.4 B7-H3.CAR-T cells control the growth of human GBM cell lines *in vivo*

(A) Schema of the xenograft murine model used to test the antitumor effects of B7-H3.CAR-T cells *in vivo*. U87-GFP-FFLuc GBM cells (1 x 10^5 cells) were inoculated into the caudate nucleus and tumor growth was monitored weekly by bioluminescence (BLI) imaging. CAR-T cells (2 x 10^6 cells) were injected intratumorally 1 week after tumor inoculation. (B) Representative images of tumor BLI. (C) Log-transformed BLI values showing the kinetics of tumor growth of each mouse (n = 9 – 11 mice/group across 3 CAR-T donors). (D) Kaplan-Meier analysis of overall survival of the treated mice. Statistical analysis was performed using the Mantel-Cox log rank test (***$p<0.0001$). (E) Representative flow cytometry plots showing the expression of GFP and B7-H3 in U87-GFP-FFLuc recurrent tumors explanted from mice treated with CAR-T cells. (F) Experimental setup of xenograft rat brain slice coculture model. (G) Representative images demonstrating U87-GFP-FFLuc and GBM-NS-GFP cells seeded on rat brain slice. (H-I) Quantification of (H) IFNγ and (I) IL-2 by ELISA in the supernatant 24 hours after coculture of CAR-T cells with U87-GFP-FFLuc cells or GBM-NS-GFP at 1:2 E:T ratio on rat brain slides. Data represent one CAR-T cell donor tested against U87-GFP-FFLuc cells or one GBM-NS-GFP line on 1 - 3 different rat brain slices. Difference in means was assessed through one-way ANOVA with Bonferroni's post-test correction (**$p<0.01$).

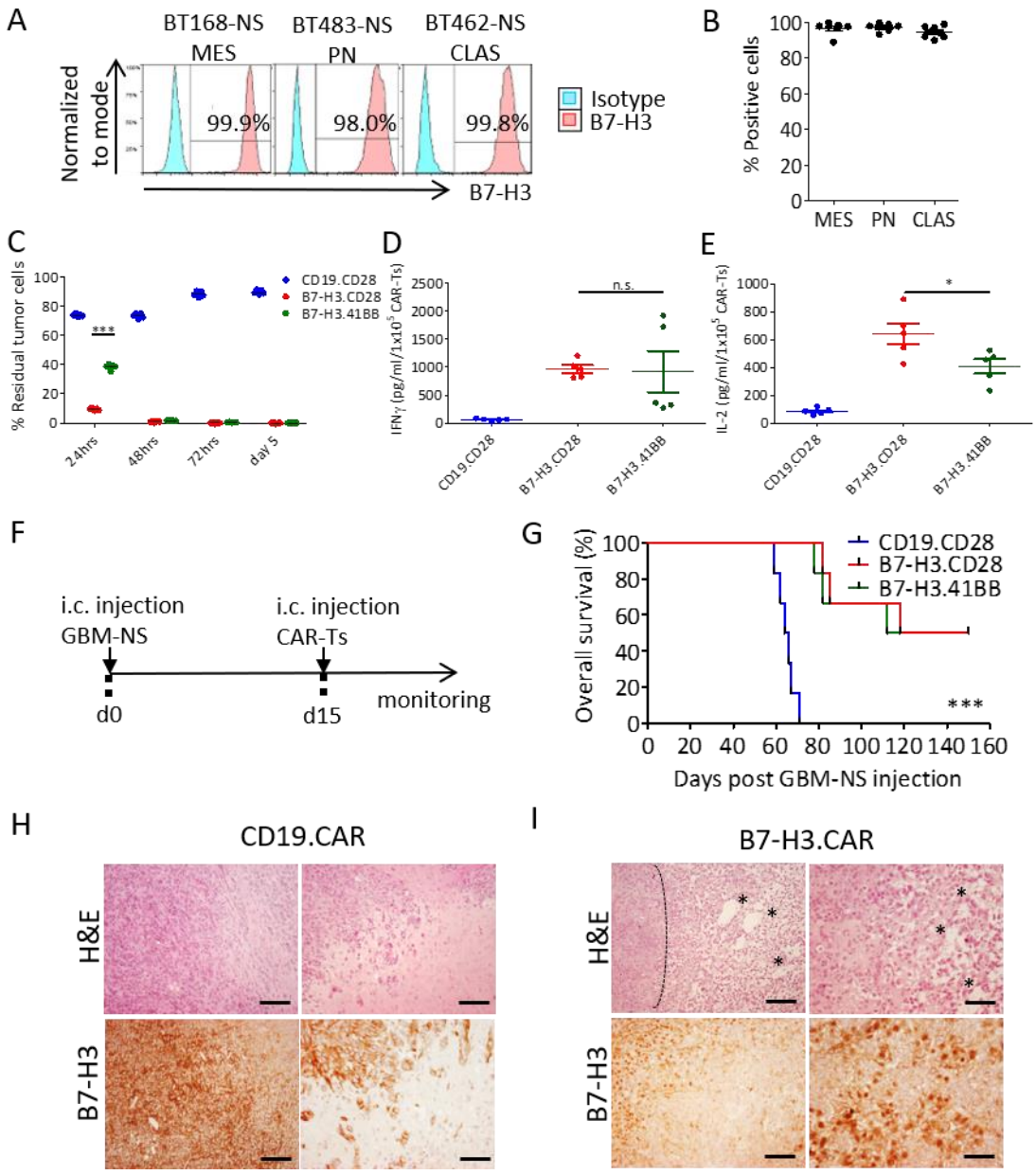

Figure 2.5 B7-H3.CAR-T cells control the growth of human GBM-NS *in vitro* and *in vivo*

(A) Representative flow plots and (B) summary plots showing B7-H3 expression in human GBM-NS as assessed by flow cytometry (n = 20). GBM-NS were subdivided by molecular subtypes (MES: mesenchymal, n = 6; PN: proneural, n = 6; CLAS: classical, n = 8). (C) CAR-T cells were co-cultured with GBM-NS at 1:5 E:T ratio and residual tumor cells (B7-H3$^+$) were quantified by flow cytometry at different time points. Data represent the average of two donors of CAR-T cells tested against five GBM-NS. Difference in means was assessed through two-way ANOVA with Bonferroni's post-test correction (***p<0.0001). (D) IFNγ and (E) IL-2 release by B7-H3.CAR-T cells and CD19.CAR-T cells in the supernatant collected 24 hours after coculture with GBM-NS.

BT166-NS and BT462-NS released higher levels of IFNγ compared to BT308-NS, BT302-NS and BT273-NS[156]. Data represent the average of two donors of CAR-T cells tested against five GBM-NS. Difference in means was assessed through one-way ANOVA with Bonferroni's post-test correction (*p<0.05). (F) Schema of the xenograft murine experimental model used to test the antitumor effects of CAR-T cells against GBM-NS. GBM-NS (1 x 10^5 cells) were inoculated into the caudate nucleus and CAR-T cells (2 x 10^6 cells) were injected intratumorally 2 week later. (G) Kaplan-Meier curves showing the overall survival of the treated mice (n = 6 mice/group). Overall survival comparison was done using the Mantel-Cox log rank test (***p<0.0001). (H,I) Morphology assessed by hematoxylin and eosin staining and B7-H3 expression assessed by immunohistochemistry of xenograft gliomas from tumor-bearing mice. (H) Gliomas collected from mice treated with CD19.CAR-T cells show high cellularity and high B7-H3 expression. (I) Gliomas collected from mice treated with B7-H3.CAR-T cells show necrotic zones with fibrotic areas (marked by asterisks) and disrupted tumor architecture. Delimited area shows dense cellularity at the borders of necrosis. Scale bar, 100 μm.

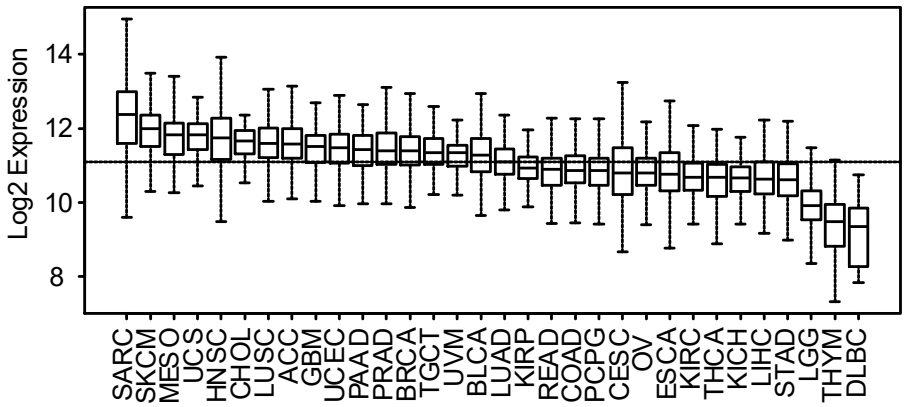

Figure S2.1 Analysis of B7-H3 mRNA expression in tumors using the TCGA data set

Expression of B7-H3 mRNA in GBM is relatively high compared to other cancers. Pan-cancer analysis of normalized B7-H3 mRNA expression in all primary tumors in TCGA. The horizontal dotted line represents the mean normalized B7-H3 mRNA expression across all tumors.

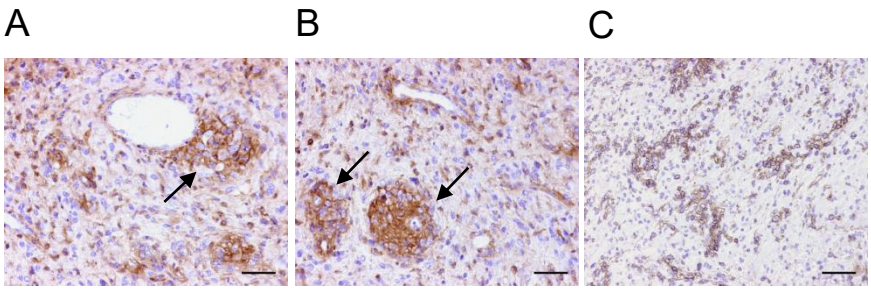

Figure S2.2 Figure 3. Distribution of B7-H3 expressing tumor cells within the tumor architecture

(A, B) Representative immunohistochemistry showing B7-H3 expressing GBM tumor cells with a migration front moving along the tumor blood vessels (A). Tumor clusters intensively positive for B7-H3 are found at the tumor edge (B). (C) Representative immunohistochemistry showing that GBM tumor cells expressing B7-H3 infiltrate the peritumoral tissue. Scale bar, 50 µm.

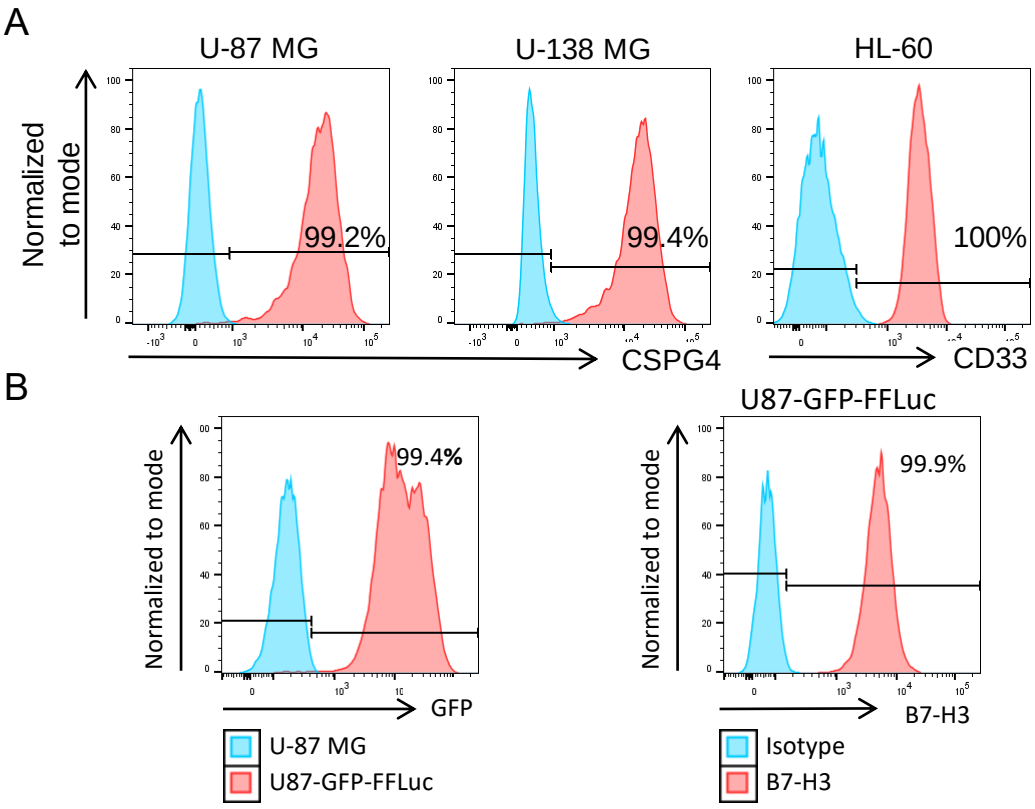

Figure S2.3 Phenotyping analysis of the tumor cell lines used for the coculture and *in vivo* experiments.

(A) Phenotyping of GBM cell lines U-87 MG and U-138 MG for CSPG4, and HL-60 for CD33. (B) Phenotyping of U-87 MG cells stably expressing *GFP-FFLuc* for GFP expression and B7-H3 antigen retention using 376.96 mAb.

Table 2.1 GBM specimen and NS classification and B7-H3 expression.

Patient ID	B7-H3 expression	GBM-NS subtype	B7-H3 expression in GBM-NS (%)
BT137	+	PN	
BT140	+	MES	
BT150	+	CLAS	
BT202	+	MES	
BT205	+	PN	98.0
BT211	+	MES	
BT219	+	MES	
BT235	+	CLAS	
BT241	+	NA	
BT245	+	PN	
BT248	+	NA	
BT302	+	MES	99.0
BT308	+	PN	98.0
BT328	+	MES	92.3
BT337	+	PN	
BT347	+	NA	
BT379	+	CLAS	94.8
BT417	+	CLAS	98.0
BT422	+	CLAS	98.4
BT423	+	CLAS	94.6
BT462	+	CLAS	99.8
BT482	+	MES	99.9
BT483	+	PN	98.0
BT513	+	MES	
BT517	+	CLAS	97.7
BT138	++	CLAS	
BT168	++	MES	99.9
BT175	++	NA	
BT275	++	CLAS	97.1
BT283	++	CLAS	
BT261	++	CLAS	
BT358	++	MES	92.1
BT373	++	PN	89.0
BT480	++	MES	
BT500	++	CLAS	
BT487	+/-	MES	96.4
BT326	+/-	PN	90.1
BT273	+/-	CLAS	97.8
BT299	+/-	PN	95.5

BT155	+/-	CLAS
BT209	+/-	PN
BT206	+/-	CLAS
BT334	+/-	CLAS
BT274	+/-	PN
BT279	+/-	CLAS
BT157	-	MES

GBM-NS: glioblastoma-neurospheres; PN: proneural; CLAS: classical; MES: mesenchymal; NA: not available

2.5 Materials and Methods

2.5.1 Analysis of The Cancer Genome Atlas (TCGA) database

The PanCan mRNA normalized data (http://api.gdc.cancer.gov/data/3586c0da-64d0-4b74-a449-5ff4d9136611) was downloaded, filtered for primary tumors and log2 transformed. The gene expression for *CD276* was then plotted by tumor type. Also, GBM samples (normal, primary tumors, and recurrent tumors) were extracted from the PanCan dataset and *CD276*, *CSPG4*, *EPHA2*, *ERBB2*, and *IL13RA2* were plotted by sample type. All analysis was performed in R.

2.5.2 GBM specimen, GBM-NS, tissue microarrays (TMAs), and cell lines

Patient GBM specimens were obtained from the Department of Neurosurgery (Istituto Neurologico Carlo Besta, Milan Italy) according to a protocol approved by the local institutional review board and upon patients' informed consent. GBM diagnosis was determined according to the WHO Classification[6]. GBM-NS were generated as previously described[176]. GBM and normal brain formalin-fixed paraffin-embedded (FFPE) TMAs were obtained from US BioMax (TMA #: GL801e, BNC17011b, GLN241). U-87 MG cells (RRID: CVCL_0022) were obtained from ATCC, U-138 MG cells (RRID: CVCL_0020) from DSMZ, and HL-60 cells (RRID: CVCL_0002) from UNC's Tissue

Culture Facility cell line repository which purchases its lines from ATCC. All cell lines were authenticated by their original vendor. U-87 MG and U-138 MG cells were grown in Dulbecco Modified Eagle Medium (DMEM) (Thermo Fisher Scientific) while HL-60 cells were grown in RPMI 1640 (Thermo Fisher Scientific) supplemented with 10% fetal bovine serum (FBS) (Gemini Bio-Products), 1% penicillin/streptomycin (Thermo Fisher Scientific), and 1% GlutaMAX™ (Thermo Fisher Scientific). Cell lines were phenotyped for B7-H3 expression using the 376.96 mAb followed by APC-goat anti-mouse (BD Biosciences), or using the B7-H3-BV421 mAb (Clone 7-517; BD Bioscience)[168]. SFG plasmid harboring green fluorescent protein and firefly luciferase genes (SFG.GFP-FFLuc) was used to generate dual GFP- and FFLuc-expressing cell lines. GBM cell lines and GBM-NS were routinely tested to confirm the absence of mycoplasma (Lonza) and for the expression of the targeted antigen by flow cytometry.

2.5.3 Immunohistochemistry

Carnoy-fixed GBM specimens, and paraffin-embedded xenograft gliomas were processed as previously described[156]. The staining was performed using the anti-B7-H3 mAb (1:200 dilution, AF1027, R&D systems). Staining was detected using an anti-goat biotin secondary mAb for 2 hour at room temperature, then a streptavidin-HRP for 1 hour and the chromogen DAB/substrate reagent for the GBM specimens and VECTASTAIN® ABC HRP Kit for xenograft gliomas. Slides were counterstained with hematoxylin (Sigma Aldrich, Inc), dehydrated and mounted. A semiquantitative analysis of B7-H3 expression was performed on 46 human GBM specimens by an experienced pathologist (BP). The expression levels were scored as < 5% positive cells or 5 - 20 % positive cells (- and +/-, respectively; low expression); as 20 - 50% positive cells and >

50% positive cells (+ and ++, respectively; high expression). GBM and normal brain TMAs were stained using the anti-B7-H3 mAb (AF1027, R&D Systems) by the Translational Pathology Lab core facility and analyzed using the Aperio software. Total IHC score for each core in the TMAs was calculated using Aperio Color Deconvolution Algorithm v9 as follows: Score = (% area with IHC score 0) x 0 + (% area with IHC score 1+) x 1 + (% area with IHC score 2+) x 2 + (% area with IHC score 3+) x 3. The score of each core was normalized to a positive control to compare stains across slides.

2.5.4 Coculture experiments

The B7-H3.CAR cassettes were generated using the single chain variable fragment (scFv) from the anti-B7-H3 376.96 mAb[168]. The control CD19.CAR was previously described[169]. CAR-T cells were generated from healthy donor peripheral blood T cells (obtained from buffy coats, Gulf Coast Regional Blood Center) as previously described[177]. B7-H3.CAR expression was assessed by incubating the CAR-T cells with B7-H3-GFP[168]. CD19.CAR expression was assessed by incubation with anti-CD19.CAR mAb[169]. To test the antitumor activity *in vitro* of CAR-T cells, tumor cells were seeded at 1 x 10^5 cells/well in tissue culture-treated plates (Corning) at either 1:5 or 1:10 effector-to-target (E:T) ratio with the CAR-T cells. CAR-T cells were plated in cytokine-free media for 24 hours before being added to the tumor cells. In each experiment, the percentage of CAR-T cells in each group was normalized to the group with the lowest CAR expression using control T cells. To measure cytokine release, the supernatant was collected 24 hours after CAR-T cell seeding. Cells were harvested non-enzymatically, using 480 μM ethylenediaminetetraacetic aicd (EDTA) (Thermo Fisher Scientific) in phosphate buffered saline (PBS) (Thermo Fisher Scientific), and

stained with an anti-CD3 mAb (clone SK7; BD Biosciences) to detect T cells, and with mAbs specific for tumor markers to detect tumor cells, and separately for viability using ZombieAqua viability dye (BioLegend). CAR-T cells and tumor cells were quantified using CountBright™ Absolute Counting Beads (Thermo Fisher Scientific). To identify the tumor cells in coculture, we used an anti-CSPG4 mAb (Clone 1E6.4; Miltenyi Biotec) for U-87 MG and U-138 MG cells, and an anti-CD33 mAb (Clone WM53; BD Biosciences) for HL-60 due to their uniform expression in their respective tumor cell lines (Fig. S2.3A). For coculture experiments with GBM-NS, cells were plated in tissue culture-treated 24-well plates (Corning) at 1:5 E:T ratio with the CAR-T cells in serum-free DMEM/F12 (Thermo Fisher Scientific) with B27™ supplement (Thermo Fisher Scientific)[156]. The supernatant was collected 24 hours after CAR-T cell seeding to measure cytokine release. Cells were harvested after 1, 2, 3, or 5 days and stained with the anti-CD3 (Clone REA613; Miltenyi Biotec) and anti-B7-H3 (Clone FM276; Miltenyi Biotec) mAbs and analyzed by flow cytometry. Interferon γ (IFNγ) and interleukin-2 (IL-2) levels in 24-hour coculture supernatant were measured in duplicates using specific enzyme-linked immunosorbent assay (ELISA) kits (R&D System) following the manufacturer's instructions. GBM-NS coculture experiments were analyzed using MACSQuant® Analyzer (Miltenyi Biotec) and FlowLogic V7.1 Software. All remaining flow cytometry experiments were acquired using FACS Canto II (BD Bioscience), and analyzed using the FlowJo software (Version 10.0). Carboxyfluorescein succinimidyl ester (CFSE) staining was performed as previously described[156].

2.5.5 Xenograft brain slice coculture model

Hemicoronal brain slices (250 μm thick) from postnatal day 8 CD Sprague Dawley rats (Charles River) were prepared using a vibratome (Leica) and placed in 6-well plates with filtered transwell inserts (Corning). The slices were maintained with 1 mL culture medium (Neurobasal-A medium supplemented with 10% heat-inactivated porcine serum, 5% heat-inactivated rat serum, 10 mM KCl, 10 mM (4-(2-hydroxyethyl)-1-piperazineethanesulfonic acid (HEPES), 100 U/ml Penicillin/Streptomycin, 1 mM Sodium Pyruvate, 1 mM L-Glutamine, and 1 μM MK801) under the filter, incubating at 37°C and 5% CO_2. HF2303 tumor nurospheres were obtained from Dr. Ana deCarvalho and the Hermelin Brain Tumor Bank at Henry Ford Health System, Detroit MI, USA. The neurospheres were infected using LV-GFP virus at 10 multiplicity of infection (MOI) with 5 μg/mL polybrene overnight and were maintained in NM medium (DMEM/F12 supplemented with, 500 μg/mL bovine serum albumin (BSA), 12.5 μg/mL gentamycin, antibiotic-antimycotic, N-2 supplement). U87-GFP-FFLuc cells were counted using Nexelcom Cellometer Auto 2000 and prepared at 10,000,000 cells/mL. HF2303-GFP cells counted using the hemacytometer were prepared at 200,000 cells/ml. Each brain slice was plated with 5 μL of respective cell suspension (50,000 U87-GFP-FFLuc cells or 10,000 HF2303-GFP cells). One hudrend μl of media from each well was collected at 24 hours after plating for cytokine analysis.

2.5.6 Xenograft mouse models

The antitumor activity of CAR-T cells was tested in *nu/nu* mice (Animal Studies Core Facility, UNC) according to an Institutional Animal Care and Use Committee (IACUC) approved protocol. Female *nu/nu* mice ages 6 - 10 weeks were injected with 1

x 10^5 U87-GFP-FFLuc cells in 3 µL PBS intracranially at the following coordinates relative to the bregma, corresponding to the caudate nucleus: 0.7 mm posteriorly, 3 mm laterally to the right, and 3.5 mm deep. A week later, tumor burden was assessed using bioluminescence (BLI) measured by the IVIS Kinetic (Caliper LifeSciences), and 2 x 10^6 CAR-T cells in 5 µL PBS were injected intratumorally. Tumor BLI was quantified weekly thereafter. Mice were monitored every 2 - 3 days, and culled upon reaching humane end points in accordance with institutional guidelines. Overall survival was assessed using Kaplan-Meier analysis. Explanted tumors were dissociated using Human Tumor Dissociation Kit (Miltenyi Biotec) as per the manufacturer's instructions. The antitumor activity against GBM-NS was tested in congruence with a locally approved protocol (Istituto Neurologico Carlo Besta, Milan, Italy) and in accordance to the Italian Principle of Laboratory Animal Care (D. Lgs. 26/2014) and European Communities Council Directives (86/609/EEC and 2010/63/UE). *Nude* (CD1 (HO): CD1-Foxn1^{nu}, from Charles River Laboratories, Calco, Italy female mice ages 6 weeks were injected intracranially at the coordinates described above with 1 x 10^5 GBM-NS cells in 2 µL PBS and, 15 days later, with 2 x 10^6 CAR-T cells in 5 µL PBS intratumorally. Mice were then monitored every 2 - 3 days and sacrificed when showing neurological symptoms and/or reduced body condition.

2.5.7 Statistical analysis

Statistical significance of the difference of means between two groups was assessed using a 2-tailed, nonparametric Mann-Whitney U test. For more than two groups, we used one-way or two-way ANOVA with Bonferroni's post-test correction. The difference in overall survival in Kaplan-Meier curves was determined using the log-

rank Mantel-Cox test. All statistical analyses were performed in GraphPrism (Version 5.03).

CHAPTER 3: GENERAL DISCUSSION

3.1 Summary

Using T cells engineered to stably express B7-H3-specific CAR, this work shows that GBM tumor cells can be effectively eliminated *in vitro* and *in vivo*. B7-H3 is not only highly expressed in our GBM cell lines and patient-derived GBM-NS, but it is importantly expressed in all but one of the GBM specimen we tested, with 76% of specimens expressing it at high levels, across molecular subtypes. This antitumor efficacy was shown both *in vitro*, in a brain slice xenograft model, and in an orthotopic xenograft murine model with durable responses and nearly no recurrences. The choice of CD28 or 4-1BB co-stimulatory domain influenced the short-term kinetics of the antitumor effect and the levels of cytokines release *in vitro*, but had no influence on the outcomes *in vivo*.

3.2 Overcoming molecular heterogeneity with B7-H3-specific CAR T cells

Failure of targeted therapies in GBM, including CAR T therapies, to produce a significant survival benefit so far is largely due to the spatiotemporal molecular heterogeneity of tumors within and across patients[49,150,153]. The variation in expression of IL13Rα2 and ErbB2 (HER2) we observed in our TCGA analysis (Fig. 2.1A) supports the clinical observations documented with CARs targeting these antigens that the tumors recur with reduced antigen expression. The variation in antigen expression across different patients can falsely suggest that the CAR is ineffective if patient

enrollment does not depend on the antigen status. This problem was seen in the design of early studies of targeted therapy in GBM, especially of EGFR inhibitors[49]. It is worth noting in this context that in the Intellance 2 clinical trial of the ADC depatux-m, the investigators confirmed EGFR-amplification and demonstrated some survival benefit (40% vs 28% 1-year survival)[68]. Thus, CAR T cell approaches that target molecules with high variability in expression across patients must be tested in patients with confirmed antigen expression to be able to draw the most informative conclusions about antitumor efficacy.

The expression of B7-H3 we observed in the TCGA data and measured in our GBM specimen and GBM-NS suggests a less heterogenous expression both intra- and intertumorally, with equally elevated expression across different molecular subtypes. Nonetheless, since CAR T cells are amenable to immunosuppressive signals, the heterogeneity in immunological microenvironment described by Doucette *et al.* can yield varying efficacies *in vivo*[69]. The mesenchymal subtype has been described as the most "immunogenic" due to the enrichment of both immune activating and inhibiting gene signatures. It is likely that B7-H3.CAR-T cells would be the least effective in this subtype due to the dominance of immunosuppression over antitumor immunity. This hypothesis could possibly be tested in an orthotopic, immunocompetent murine model of GBM.

As mentioned previously, the low expression of B7-H3 on about a quarter of the primary GBM quantified raises concerns regarding the efficacy of B7-H3.CAR-T cells for these patients, as demonstrated in preclinical studies of CSPG4-specific CAR T cells[156]. These cases may necessitate multiple treatment modalities to effectively control tumor growth. Since both B7-H3 and CSPG4 both show elevated expression levels in GBM

with relatively lower variance, co-targeting of these antigens using either doubly-transduced CAR T cells, a bispecific CAR, or two CAR T cell populations can improve response. There are several challenges in these approaches, however. T cells transduced with two CAR constructs may have lower transduction efficiency and the two CARs may compete for signaling molecules necessary for T cell activation. Overactivation of the T cells may also lead to expedited exhaustion and thus reduced efficacy; choosing an appropriate T cell subset and co-stimulatory domain(s) will be necessary to mitigate this problem. There is also an increased chance of malignant transformation, or functional impairment, of the T cells due to insertional mutagenesis. A bispecific CAR can may overcome these issues by reducing competition for signaling molecules and reducing the likelihood of excess insertional mutagenesis, but a design of such CAR construct can be challenging. A bispecific CAR will have to be a larger construct which, depending on the size, could be challenging to package in the virus. Larger CAR constructs also reduce the transduction efficiency. Finally, using two CAR T cell populations is bound to be extremely cost-prohibitive.

Studies into the specific molecular mechanisms by which B7-H3.CAR-T cells eliminate tumors can further help us understand how they can overcome molecular heterogeneity. Our group has previously shown that CD30-redirected CAR T cells for embryonal carcinoma can eliminate tumors both in an antigen-dependent manner through CAR-mediated target recognition, and through an antigen-independent manner via Fas/FasL engagement, leading to cell death in both CD30+ and CD30- tumor cells[178]. This passerby antitumor effect will be useful in the clearance of B7-H3-negative or -low GBM cells, if in fact it is employed.

3.3 Delivery of CAR T cells in GBM

The advantage of being able to deliver CAR T cells intracranially into the tumor or the ventricle system should not be understated[161]. The standard route of administration of CAR T cells is intravenously, which requires the T cells to traffic to the tumor. Tumors may employ various mechanisms to suppress T cell migration into the tumor[179]. Intratumoral delivery bypasses this obstacle and allows for enrichment of CAR T cells at the target. This can be particularly useful in cases of large tumors, where it would be difficult for the T cells to penetrate through the tumors. Delivery into the ventricular system has surprisingly proven to be very effective for multifocal cases[161]. GBM has been shown to travel along white matter tracts, and IHC staining from our study indicates vasculature-bordering, B7-H3-intense tumor cells. Thus, there could be multiple routes through which GBM spreads locally. It would be worthy to evaluate multi-route delivery of either the same or different CAR T cells to address all the possible dissemination routes of the tumor.

3.4 Targeting CSCs with B7-H3.CAR-T cells

The ubiquitous and high expression of B7-H3 in our GBM-NS (Fig. 2.5A, B, Table 2.1) along with the successful elimination of patient-derived GBM-NS across all molecular subtypes (Fig. 2.5) is an encouraging sign that CSC can be successfully targeted[167]. It is nevertheless expected that CSCs with absent-to-low expression of B7-H3 could escape targeting by B7-H3.CAR-T cells and contribute to recurrence. This therapy-induced clonal selection was specifically demonstrated in matched pairs of CSCs from primary and recurrent GBM from patients treated with TMZ or

radiochemotherapy [166]. Eliminating CSCs not only can potentially limit progression and recurrence[172], but given the interplay of CSCs with M2 macrophages[107], it can also promote a more immunopermissive environment that will propagate further antitumor immunity. This concept can be best explored by comparison of GBM models of the two most immunologically dissimilar subtypes: the immune-rich mesenchymal and immune-deprived proneural. Targeting CSCs could be the most effective way to stop tumor progression and improve survival, since CSCs are often treatment-resistant and are central for progression.

3.5 Conclusions and future directions

There are a few important drawbacks in our stud that need to be addressed in future studies. One of the hallmarks of human GBM is its early invasive and diffusive nature, a feature that makes it essentially incurable via surgical resection and can contribute to tumor progression and recurrence[10]. The orthotopic xenograft cell line model used in our study does not grow invasively, thereby facilitating tumor elimination by the CAR T cells. It also precludes us from studying the ability of intratumoral CAR T cell delivery to engage in regions with relatively low tumor-to-normal tissue ratio. Moreover, using an invasive GBM model would also allow us to test the potential of CAR T delivery into the resection cavity and preventing recurrence. Since newly diagnosed GBM patients undergo surgical resection when possible, these studies can provide highly translational data. Our data shows that B7-H3 is highly expressed at tumor invasive edges and in vasculature-proximal tumor cell (Fig. S2.2), hence the delivery of B7-H3.CAR-T cells to the resection cavity may be a promising approach to prevent tumor recurrence and locoregional spread.

Testing the B7-H3.CAR-T cells on an orthotopic GBM model in immunocompetent mice is of utter importance. Various immunosuppressive cells, such as M2 macrophages, MDSCs, and T_{reg} are thought to contribute to the tumor microenvironment in GBM[104,107,114], and their effect on tumor elimination by CAR T cells in preclinical models can help optimize the culture conditions and CAR construct to maximize efficacy and persistence based on the tumor microenvironment. To that end, our group is in the process of testing the benefit of adding an element to that CAR construct that disrupts the PD-1/PD-L1 axis, since PD-L1 is known to be upregulated in GBM, especially in the mesenchymal subtype[117].

The work presented in this dissertation supports the use of B7-H3-redirected CAR T cells for the treatment of GBM. We show that B7-H3 is a targetable antigen that is superior in its expression profile relative to antigen currently targeted with CARs due to its consistently elevated expression relative to normal brain, relatively small variation across tumors, and indiscriminately elevated expression across molecular subtypes. Furthermore, our data suggests that B7-H3 CAR T cells can eliminate GBM cell lines and GBM-NS *in vitro*, in brain tissue xenograft models, and in orthotopic xenograft murine models. Our models suggested only limited superiority of CD28-co-stimulated B7-H3 CAR *in vitro* that did not translate into survival benefit *in vivo*. Using CAR T cell technology to target B7-H3 in GBM is an attractive approach that should be further investigated, especially in the context of the immune microenvironment across different molecular subtypes and the benefit of targeting CSCs in addition to more differentiated GBM tumor cells.

REFERENCES

1. Hanif, F., Muzaffar, K., Perveen, K., Malhi, S. M. & Simjee, S. U. Glioblastoma Multiforme: A Review of its Epidemiology and Pathogenesis through Clinical Presentation and Treatment. *Asian Pacific J. Cancer Prev.* **18**, 3–9 (2017).

2. Ostrom, Q. T. *et al.* CBTRUS Statistical Report: Primary Brain and Other Central Nervous System Tumors Diagnosed in the United States in 2011–2015. *Neuro. Oncol.* **20**, iv1–iv86 (2018).

3. Alexander, B. M. & Cloughesy, T. F. Adult glioblastoma. *J. Clin. Oncol.* **35**, 2402–2409 (2017).

4. Stupp, R. *et al.* Radiotherapy plus concomitant and adjuvant temozolomide for glioblastoma. *N. Engl. J. Med.* **352**, 987–96 (2005).

5. Ohgaki, H. Genetic Pathways to Primary and Secondary Glioblastoma. *Am. J. Patholo* **170**, 1445–1453 (2007).

6. Louis, D. N. *et al.* The 2016 World Health Organization Classification of Tumors of the Central Nervous System: a summary. *Acta Neuropathol* (2016). doi:10.1007/s00401-016-1545-1

7. Dietrich, A. J. UpToDate: Clinical presentation, initial surgical approach, and prognosis of high-grade gliomas. (2019).

8. Norden, A. D. & Wen, P. Y. Glioma Therapy in Adults. *Neurologist* **12**, 279–292 (2006).

9. Mittal, S. *et al.* Alternating electric tumor treating fields for treatment of glioblastoma: rationale, preclinical, and clinical studies. *J Neurosurg* **128**, 414–421 (2018).

10. Gieryng, A., Pszczolkowska, D., Walentynowicz, K. A., Rajan, W. D. & Kaminska, B. Immune microenvironment of gliomas. *Lab. Investig.* **97**, 498–518 (2017).

11. Pitter, K. L. *et al.* Corticosteroids compromise survival in glioblastoma. *Brain* **139**, 1458–1471 (2016).

12. Klement, R. J. & Champ, C. E. Corticosteroids compromise survival in glioblastoma in part through their elevation of blood glucose levels. *Brain* **140**, 1–2 (2017).

13. Stupp, R. *et al.* NovoTTF-100A versus physician's choice chemotherapy in recurrent glioblastoma: A randomised phase III trial of a novel treatment modality. *Eur. J. Cancer* **48**, 2192–2202 (2012).

14. Stupp, R. *et al.* Maintenance Therapy With Tumor-Treating Fields Plus Temozolomide vs Temozolomide Alone for Glioblastoma: A Randomized Clinical Trial. *J. Am. Med. Assoc.* **314**, 2535–2543 (2015).

15. Rubenstein, J. L. *et al.* Anti-VEGF antibody treatment of glioblastoma prolongs survival but results in increased vascular cooption. *Neoplasia* **2**, 306–14 (2000).

16. Chaudhry, I. H., Donovan, O. D. G., Brenchley, P. E. C., Reid, H. & Roberts, I. S. D. Vascular endothelial growth factor expression correlates with tumour grade and vascularity in gliomas. *Histopathology* **39**, 409–415 (2001).

17. Kreisl, T. N. *et al.* Phase II trial of single-agent bevacizumab followed by bevacizumab plus irinotecan at tumor progression in recurrent glioblastoma. *J. Clin. Oncol.* **27**, 740–745 (2009).

18. Vredenburgh, J. J. *et al.* Corticosteroid Use in Patients with Glioblastoma at First or Second Relapse Treated with Bevacizumab in the BRAIN Study. *Oncologist* **15**, 1329–1334 (2010).

19. Taal, W. *et al.* Single-agent bevacizumab or lomustine versus a combination of bevacizumab plus lomustine in patients with recurrent glioblastoma (BELOB trial): A randomised controlled phase 2 trial. *Lancet Oncol.* **15**, 943–953 (2014).

20. Wick, W. *et al.* Lomustine and Bevacizumab in Progressive Glioblastoma. *N. Engl. J. Med.* **377**, 1954–1963 (2017).

21. Song, J., Xue, Y. Q., Zhao, M. M. & Xu, P. Effectiveness of lomustine and bevacizumab in progressive glioblastoma: A meta-analysis. *Onco. Targets. Ther.* **11**, 3435–3439 (2018).

22. Pàez-ribes, M. *et al.* Angiogenic Therapy Elicits Malignant Progression of Tumors to Increased Local Invasion and Distant Metastasis. *Cancer Cell* **15**, 220–231 (2010).

23. Du, R. *et al.* HIF1α Induces the Recruitment of Bone Marrow-Derived Vascular Modulatory Cells to Regulate Tumor Angiogenesis and Invasion. *Cancer Cell* **13**, 206–220 (2008).

24. Piao, Y. *et al.* Glioblastoma resistance to anti-VEGF therapy is associated with myeloid cell infiltration, stem cell accumulation, and a mesenchymal phenotype. *Neuro. Oncol.* **14**, 1379–1392 (2012).

25. Molenaar, R. J. *et al.* The combination of IDH1 mutations and MGMT methylation status predicts survival in glioblastoma better than either IDH1 or MGMT alone. *Neuro. Oncol.* **16**, 1263–1273 (2014).

26. Parsons, D. W. *et al.* An Integrates Genomic Analysis of Human Glioblastoma Multiforme. *Science (80-.).* **321**, 1807 (2008).

27. Gerson, S. L. MGMT: Its role in cancer aetiology and cancer therarpeutics. *Nat. Rev. Cancer* **4**, 296–307 (2004).

28. Weiler, M. *et al.* mTOR target NDRG1 confers MGMT-dependent resistance to alkylating chemotherapy. *Proc. Natl. Acad. Sci.* **111**, 409–414 (2014).

29. Yan, H. *et al.* IDH1 and IDH2 Mutations in Gliomas. *N. Engl. J. Med.* **360**, 765–773 (2009).

30. Tran, A. N. *et al.* Increased sensitivity to radiochemotherapy in IDH1 mutant glioblastoma as demonstrated by serial quantitative MR volumetry. *Neuro. Oncol.* **16**, 414–420 (2014).

31. Hata, N. *et al.* Insular primary glioblastomas with IDH mutations: Clinical and biological specificities. *Neuropathology* **37**, 200–206 (2017).

32. Ohgaki, H. & Kleihues, P. The definition of primary and secondary glioblastoma. *Clin. Cancer Res.* **19**, 764–772 (2013).

33. Cohen, A., Holmen, S. & Colman, H. IDH1 and IHD2 Mutations in Gliomas. *Curr. Neurol. Neurosci. Rep.* **13**, 345 (2013).

34. Zhao, S. *et al.* Glioma-Derived Mutations in IDH1 Dominantly Inhibit IDH1 Catalytic Activity and Induce HIF-1α Shimin. *Science (80-.).* **324**, 261–265 (2009).

35. Jin, G. *et al.* 2-Hydroxyglutarate Production, but Not Dominant Negative Function, Is Conferred by Glioma-Derived NADP+ -Dependent Isocitrate Dehydrogenase Mutations. *PLoS One* **6**, e16812 (2011).

36. Brennan, C. W. *et al.* The Somatic Genomic Landscape of Glioblastoma. *Cell* **155**, 462–477 (2013).

37. Phillips, H. S. *et al.* Molecular subclasses of high-grade glioma predict prognosis, delineate a pattern of disease progression, and resemble stages in neurogenesis. *Cancer Cell* **9**, 157–173 (2006).

38. Roel G.W. Verhaak1, 2 *et al.* An integrated genomic analysis identifies clinically relevant subtypes of glioblastoma characterized by abnormalities in PDGFRA, IDH1, EGFR and NF1. *Cancer Cell* **17**, 38–46 (2010).

39. Verhaak, R. G. W. *et al.* An integrated genomic analysis identifies clinically relevant subtypes of glioblastoma characterized by abnormalities in PDGFRA, IDH1, EGFR, and NF1. *Cancer Cell* **17**, 98–110 (2010).

40. Lottaz, C. *et al.* Transcriptional profiles of CD133+ and CD133- glioblastoma-derived cancer stem cell lines suggest different cells of origin. *Cancer Res.* **70**, 2030–2040 (2010).

41. Kong, J. *et al.* Integrative, Multi-modal Analysis of Glioblastoma Using TCGA Molecular Data, Pathology Images and Clinical Outcomes. *IEEE Trans Biomed Eng* **58**, 3469–3474 (2011).

42. Kim, Y. *et al.* Identification of prognostic gene signatures data analysis. *Neuro. Oncol.* **15**, 829–839 (2013).

43. Noushmehr, H. *et al.* Identification of a CpG Island Methylator Phenotype that Defines a Distinct Subgroup of Glioma. *Cancer Cell* **17**, 510–522 (2010).

44. Sandmann, T. *et al.* Patients With Proneural Glioblastoma May Derive Overall Survival Bene fi t From the Addition of Bevacizumab to First-Line Radiotherapy and Temozolomide: Retrospective Analysis of the AVAglio Trial. *J. Clin. Oncol.* **33**, 2735–2744 (2015).

45. Snuderl, M. *et al.* Mosaic amplification of multiple receptor tyrosine kinase genes in glioblastoma. *Cancer Cell* **20**, 810–817 (2011).

46. Sottoriva, A. *et al.* Intratumor heterogeneity in human glioblastoma reflects cancer evolutionary dynamics. *Proc. Natl. Acad. Sci.* **110**, 4009–4014 (2013).

47. Patel, A. P. *et al.* Single-cell RNA-seq highlights intratumoral heterogeneity in primary glioblastoma. *Science (80-.).* **344**, 1396–1401 (2014).

48. Reardon, D. A., Wen, P. Y. & Mellinghoff, I. K. Targeted molecular therapies against epidermal growth factor receptor: Past experiences and challenges. *Neuro. Oncol.* **16**, viii7–viii13 (2014).

49. Touat, M., Idbaih, A., Sanson, M. & Ligon, K. L. Glioblastoma targeted therapy : updated approaches from recent biological insights. *Ann. Oncol.* **28**, 1457–1472 (2017).

50. Zahonero, C. & Sánchez-Gómez, P. EGFR-dependent mechanisms in glioblastoma: Towards a better therapeutic strategy. *Cell. Mol. Life Sci.* **71**, 3465–3488 (2014).

51. Lassman, A. B. *et al.* Molecular Study of Malignant Gliomas Treated with Epidermal Growth Factor Receptor Inhibitors: Tissue Analysis from North American Brain Tumor Consortium Trials 01-03 and 00-01. *Clin. Cancer Res.* **11**, 7841–7851 (2005).

52. de Vries, N. A. *et al.* Restricted brain penetration of the tyrosine kinase inhibitor erlotinib due to the drug transporters P-gp and BCRP. *Invest New Drugs* **30**, 443–449 (2012).

53. Hegi, M. E. *et al.* Pathway Analysis of Glioblastoma Tissue after Preoperative Treatment with the EGFR Tyrosine Kinase Inhibitor Gefitinib — A Phase II Trial. *Mol. Cancer Ther.* **10**, 1102–1112 (2011).

54. Vivanco, I. *et al.* Differential sensitivity of glioma- versus lung cancer-specific EGFR mutations to EGFR kinase inhibitors. *Cancer Discov.* **2**, 458–471 (2012).

55. Sepúlveda-Sánchez, J. M. *et al.* Phase II trial of dacomitinib, a pan-human EGFR tyrosine kinase inhibitor, in recurrent glioblastoma patients with EGFR amplification. *Neuro. Oncol.* **19**, 1522–1531 (2017).

56. Mellinghoff, I. K. *et al.* Molecular Determinants of the Response of Glioblastomas to EGFR Kinase Inhibitors. *N. Engl. J. Med.* **353**, 2012–2025 (2005).

57. Stommel, J. M. *et al.* Coactivation of Receptor Tyrosine Kinases Affects the Response of Tumor Cells to Targeted Therapies. *Science (80-.).* **318**, 287–291 (2007).

58. Lassman, A. B. *et al.* Phase 2 trial of dasatinib in target-selected patients with recurrent glioblastoma (RTOG 0627). *Neuro. Oncol.* **17**, 992–998 (2015).

59. Razis, E. *et al.* Phase II Study of Neoadjuvant Imatinib in Glioblastoma: Evaluation of Clinical and Molecular Effects of the Treatment. *Clin. Cancer Res.* **15**, 6258–6267 (2009).

60. Wen, P. Y. *et al.* Buparlisib in Patients With Recurrent Glioblastoma Harboring Phosphatidylinositol 3-Kinase Pathway Activation: An Open-Label, Multicenter, Multi-Arm, Phase II Trial. *J. Clin. Oncol.* **37**, (2019).

61. Massacesi, C. *et al.* PI3K inhibitors as new cancer therapeutics: implications for clinical trial design. *Onco. Targets. Ther.* **9**, 203–210 (2016).

62. Weller, M. *et al.* Rindopepimut with temozolomide for patients with newly diagnosed, EGFRvIII-expressing glioblastoma (ACT IV): a randomised, double-blind , international phase 3 trial. *Lancet Oncol.* **18**, 1373–85 (2017).

63. Nduom, E. K., Weller, M. & Heimberger, A. B. Immunosuppressive mechanisms in glioblastoma. *Neuro. Oncol.* **17**, vii9–vii14 (2015).

64. Sampson, J. H. *et al.* Immunologic Escape After Prolonged Progression-Free Survival With Epidermal Growth Factor Receptor Variant III Peptide Vaccination in Patients With Newly Diagnosed Glioblastoma. *J. Clin. Oncol.* **28**, 4722–4729 (2010).

65. Liu, Z. *et al.* Tumor-infiltrating lymphocytes (TILs) from patients with glioma. *Oncoimmunology* **6**, (2017).

66. van den Bent, M. *et al.* Efficacy of depatuxizumab mafodotin (ABT-414) monotherapy in patients with EGFR-amplified, recurrent glioblastoma: results from a multi-center, international study. *Cancer Chemother. Pharmacol.* **80**, 1209–1217 (2017).

67. Seaman, S. *et al.* Eradication of Tumors through Simultaneous Ablation of CD276/B7-H3 Positive Tumor Cells and Tumor Vasculature. *Cancer Cell* **31**, 501–515 (2017).

68. Bent, M. J. Van Den *et al.* Updated results of the INTELLANCE 2/EORTC trial 1410 randomized phase II study on Depatux-M alone, Depatux-M in combination with temozolomide (TMZ) and either TMZ or lomustine (LOM) in recurrent EGFR amplified glioblastoma (NCT02343406). *J. Clin. Oncol.* **36**, 2023 (2018).

69. Doucette, T. *et al.* Immune Heterogeneity of Glioblastoma Subtypes: Extrapolation from the Cancer Genome Atlas. *Cancer Immunol. Res.* **1**, (2013).

70. Burnet, F. M. The concept of immunological surveillance. *Prog Exp Tumor Res* **13**, 1–27 (1970).

71. Dunn, G. P., Bruce, A. T., Ikeda, H., Old, L. J. & Schreiber, R. D. Cancer immunoediting: from immunosurveillance to tumor escape. *Nat. Immunol.* **3**, 991–8 (2002).

72. Shankaran, V. *et al.* IFNγ, and lymphocytes prevent primary tumour development and shape tumour immunogenicity. *Nature* **410**, 1107–1111 (2001).

73. Mittal, D., Gubin, M. M., Schreiber, R. D. & Smyth, M. J. New insights into cancer immunoediting and its three component phases - elimination, equilibrium and escape. *Curr. Opin. Immunol.* **27**, 16–25 (2014).

74. Kim, H.-J. & Cantor, H. CD4 T-cell Subsets and Tumor Immunity: The Helpful and the Not-so-Helpful. *Cancer Immunol. Res.* **2**, 91–98 (2014).

75. Reiser, J. & Banerjee, A. Effector, Memory, and Dysfunctional CD8 + T Cell Fates in the Antitumor Immune Response . *J. Immunol. Res.* **2016**, 1–14 (2016).

76. Sarantopoulos, S., Lu, L. & Cantor, H. Qa-1 restriction of CD8+ suppressor T cells. *J. Clin. Invest.* **114**, 1218–1221 (2004).

77. Quezada, S. A. *et al.* Tumor-reactive CD4 + T cells develop cytotoxic activity and eradicate large established melanoma after transfer into lymphopenic hosts . *J. Exp. Med.* **207**, 637–650 (2010).

78. Ngoenkam, J., Schamel, W. W. & Pongcharoen, S. Selected signalling proteins recruited to the T-cell receptor–CD3 complex. *Immunology* **153**, 42–50 (2018).

79. Chen, L. & Flies, D. B. Molecular mechanisms of T cell co-stimulation and co-inhibition. *Nat Rev Immunol* **13**, 227–242 (2013).

80. Zhang, H. *et al.* 4-1BB Is Superior to CD28 Costimulation for Generating CD8+ Cytotoxic Lymphocytes for Adoptive Immunotherapy. *PLoS One* **179**, 4910–4918 (2007).

81. Curtsinger, J. M. & Mescher, M. F. Inflammatory Cytokines as a Third Signal for T Cell Activation. *Curr Opin Immunol* **22**, 333–340 (2010).

82. Waterhouse, N. J., Sedelies, K. A. & Trapani, J. A. Role of Bid-induced mitochondrial outer membrane permeabilization in granzyme B-induced apoptosis. *Immunol. Cell Biol.* **84**, 72–78 (2006).

83. Li, X. Y., Li, Z., An, G. J., Liu, S. & Lai, Y. D. Co-expression of perforin and granzyme B genes induces apoptosis and inhibits the tumorigenicity of laryngeal cancer cell line Hep-2. *Int. J. Clin. Exp. Pathol.* **7**, 978–986 (2014).

84. Ikeda, H., Old, L. J. & Schreiber, R. D. The roles of IFNγ in protection against tumor development and cancer immunoediting. *Cytokine Growth Factor Rev.* **13**, 95–109 (2002).

85. Rossin, Miloro & Hueber. TRAIL and FasL Functions in Cancer and Autoimmune Diseases: Towards an Increasing Complexity. *Cancers (Basel).* **11**, 639 (2019).

86. Hewitt, E. W. The MHC class I antigen presentation pathway: strategies for viral immune evasion. *Immunology* **110**, 163–169 (2003).

87. Embgenbroich, M. & Burgdorf, S. Current concepts of antigen cross-presentation. *Front. Immunol.* **9**, (2018).

88. Vigneron, N. Human Tumor Antigens and Cancer Immunotherapy. *Biomed Res. Int.* **2015**, 1–17 (2015).

89. Xiao, Y. S. *et al.* Combination of Intratumoral Invariant Natural Killer T Cells and Interferon-Gamma Is Associated with Prognosis of Hepatocellular Carcinoma after Curative Resection. *PLoS One* **8**, (2013).

90. Geissler, K. *et al.* Immune signature of tumor infiltrating immune cells in renal cancer. *Oncoimmunology* **4**, 985082 (2015).

91. Pylayeva-Gupta, Y. *et al.* IL35-producing b cells promote the development of pancreatic neoplasia. *Cancer Discov.* **6**, 247–255 (2016).

92. Meraviglia, S. *et al.* Distinctive features of tumor-infiltrating γδ T lymphocytes in human colorectal cancer. *Oncoimmunology* **6**, (2017).

93. Liu, Y. & Cao, X. Intratumoral dendritic cells in the anti-tumor immune response. *Cell. Mol. Immunol.* **12**, 387–390 (2015).

94. Kaunisto, A. *et al.* NFAT1 promotes intratumoral neutrophil infiltration by regulating IL8 expression in breast cancer. *Mol. Oncol.* **9**, 1140–1154 (2015).

95. Shou, D. *et al.* Suppressive role of myeloid-derived suppressor cells (MDSCs) in the microenvironment of breast cancer and targeted immunotherapies. *Oncotarget* **7**, (2016).

96. Falleni, M. *et al.* M1 and M2 macrophages' clinicopathological significance in cutaneous melanoma. *Melanoma Res.* **27**, 200–210 (2017).

97. Katanov, C. *et al.* Regulation of the inflammatory profile of stromal cells in human breast cancer: Prominent roles for TNF-α and the NF-κB pathway. *Stem Cell Res. Ther.* **6**, 1–17 (2015).

98. Kumar, V. *et al.* Cancer-associated fibroblasts neutralize the anti-tumor effect of CSF1 receptor blockade by inducing PMN-MDSC infiltration of tumors. *Cancer Cell* **32**, 654–668 (2017).

99. Bindea, G. *et al.* Spatiotemporal dynamics of intratumoral immune cells reveal the immune landscape in human cancer. *Immunity* **39**, 782–795 (2013).

100. Sato, E. *et al.* Intraepithelial CD8+ tumor-infiltrating lymphocytes and a high CD8+/regulatory T cell ratio are associated with favorable prognosis in ovarian cancer. *Proc. Natl. Acad. Sci.* **102**, 18538–18543 (2005).

101. Domingos-Pereira, S. *et al.* ILC2-modulated T cell–to-MDSC balance is associated with bladder cancer recurrence. *J. Clin. Invest.* **127**, 2916–2929 (2017).

102. Lué, A. *et al.* Neutrophil-to-lymphocyte ratio predicts survival in European patients with hepatocellular carcinoma administered sorafenib. *Oncotarget* **8**, 103077–103086 (2017).

103. Hussain, S. F. *et al.* The role of human glioma-infiltrating microglia/macrophages in mediating antitumor immune responses1. *Neuro. Oncol.* **8**, 261–279 (2006).

104. Andaloussi, A. El & Lesniak, M. S. An increase in CD4+CD25+FOXP3+ regulatory T cells in tumor-infiltrating lymphocytes of human glioblastoma multiforme1. *Neuro. Oncol.* **8**, 234–243 (2006).

105. Wainwright, D. A., Sengupta, S., Han, Y. & Lesniak, M. S. Thymus-derived rather than tumor-induced regulatory T cells predominate in human and experimental mouse brain tumors. *Neuro. Oncol.* **13**, 1308–1323 (2011).

106. Komohara, Y., Fujiwara, Y., Ohnishi, K. & Takeya, M. Tumor-associated macrophages: Potential therapeutic targets for anti-cancer therapy. *Adv. Drug Deliv. Rev.* **99**, 180–185 (2016).

107. Y Komohara, K Ohnishi, J Kuratsu & M Takeya1. *Possible involvement of the M2 anti-inflammatory\nmacrophage phenotype in growth of human gliomas*. *Journal of Pathology* **216**, (2008).

108. Doucette, T. A. *et al.* Signal transducer and activator of transcription 3 promotes angiogenesis and drives malignant progression in glioma. *Neuro. Oncol.* **14**, 1136–1145 (2012).

109. A., W. *et al.* Glioma cancer stem cells induce immune suppressive macrophages/microglia. *Neuro. Oncol.* **12**, iv29 (2010).

110. An, Z. *et al.* EGFR cooperates with EGFRvIII to recruit macrophages in glioblastoma. *Cancer Res.* **78**, 6785–6794 (2018).

111. P., V. *et al.* Monocytes/macrophages support mammary tumor invasivity by co-secreting lineage-specific EGFR ligands and a STAT3 activator. *BMC Cancer* **13**, no pagination (2013).

112. Gabrilovich, D. Myeloid-derived suppressor cells. *Cancer Immunol. Res.* **5**, 3–8 (2017).

113. Gabrilovich, D., Ostrand-Rosenberg, S. & Bronte, V. Coordinated regulation of myeloid cells by tumours. *Nat Rev Immunol* **12**, 253–268 (2012).

114. Gielen, P. R. *et al.* Increase in Both CD14-Positive and CD15-Positive Myeloid-Derived Suppressor Cell Subpopulations in the Blood of Patients with Glioma but Predominance of CD15-Positive Myeloid-Derived Suppressor Cells in Glioma Tissue. *J. Neuropathol. Exp. Neurol.* **74**, 390–400 (2015).

115. Jansen, T. *et al.* the Antiglioma Immune Response. **12**, 482–489 (2010).

116. Roth, P. *et al.* Malignant glioma cells counteract antitumor immune responses through expression of lectin-like transcript-1. *Cancer Res.* **67**, 3540–3544 (2007).

117. Berghoff, A. S. *et al.* Programmed death ligand 1 expression and tumor-infiltrating lymphocytes in glioblastoma. *Neuro. Oncol.* **17**, 1064–1075 (2015).

118. Parsa, A. T. *et al.* Loss of tumor suppressor PTEN function increases B7-H1 expression and immunoresistance in glioma. *Nat. Med.* **13**, 84–88 (2007).

119. Chapoval, A. I. *et al.* B7-H3: A costimulatory molecule for T cell activation and IFN-γ production. *Nat. Immunol.* **2**, 269–274 (2001).

120. Prasad, D. V. R. *et al.* Murine B7-H3 Is a Negative Regulator of T Cells. *J. Immunol.* **173**, 2500–2506 (2004).

121. Janakiram, M. *et al.* The third group of the B7-CD28 immune checkpoint family: HHLA2, TMIGD2, B7x and B7-H3. *Immunol Rev* **276**, 26–39 (2017).

122. Kraan, J. *et al.* Endothelial CD276 (B7-H3) expression is increased in human malignancies and distinguishes between normal and tumour-derived circulating endothelial cells. *Br J Cancer* **111**, 149–156 (2014).

123. Zhang, J. *et al.* B7H3 regulates differentiation and serves as a potential biomarker and theranostic target for human glioblastoma. *Lab. Investig.* (2019). doi:10.1038/s41374-019-0238-5

124. Lemke, D. *et al.* Costimulatory Protein 4IgB7H3 Drives the Malignant Phenotype of Glioblastoma by Mediating Immune Escape and Invasiveness. *Clin. Cancer Res.* **18**, 105–117 (2011).

125. Saha, D., Martuza, R. L. & Rabkin, S. D. Oncolytic herpes simplex virus immunovirotherapy in combination with immune checkpoint blockade to treat glioblastoma. *Immunotherapy* **10**, 2018–2020 (2018).

126. Xu, B. *et al.* An oncolytic herpes virus expressing E-cadherin resists NK cell clearance and improves viral spread and glioblastoma virotherapy. *Nat. Biotechnol.* (2018).

127. Dotti, G., Gottschalk, S., Savoldo, B. & Brenner, M. K. Design and Development of Therapies using Chimeric Antigen Receptor-Expressing T cells. *Immunol Rev* **257**, (2014).

128. Zhao, J., Lin, Q., Song, Y. & Liu, D. Universal CARs, universal T cells, and universal CAR T cells. *J. Hematol. Oncol.* **11**, 25–29 (2018).

129. Martyniszyn, A., Krahl, A., Andre, M. C., Hombach, A. A. & Abken, H. CD20-CD19 Bispecific CAR T Cells for the Treatment of B-Cell Malignancies. *Hum. Gene Ther.* **28**, 1147–1157 (2017).

130. Fedorov, V. D., Themeli, M. & Sadelain, M. PD-1- and CTLA-4-Based Inhibitory Chimeric Antigen Receptors (iCARs) Divert Off-Target Immunotherapy Responses. *Sci. Transl. Med.* **5**, (2013).

131. Roybal, K. T. *et al.* Engineering T cells with Customized Therapeutic Response Programs Using Synthetic Notch Receptors. *Cell* **167**, 419–432 (2016).

132. Roybal, K. T. *et al.* Precision Tumor Recognition by T Cells With Combinatorial Antigen-Sensing Circuits. *Cell* **164**, 770–779 (2016).

133. Pan, Y., Trojan, J., Guo, Y. & Anthony, D. D. Rescue of MHC-1 Antigen Processing Machinery by Down-Regulation in Expression of IGF-1 in Human Glioblastoma Cells. *PLoS One* **8**, e58428 (2013).

134. Zou, J. *et al.* Human Glioma-Induced Immunosuppression Involves Soluble Factor(s) That Alters Monocyte Cytokine Profile and Surface Markers. *J. Immunol.* **162**, 4882–4892 (1999).

135. Wu, A.-H., Wang, Y.-J., Zhang, X. & Low, W. C. Expression of Immune-Related Molecules in Glioblastoma Multiform Cells. *Chinese J. Cancer Res.* **15**, 112–115 (2003).

136. Shalabi, H. *et al.* Sequential loss of tumor surface antigens following chimeric antigen receptor T-cell therapies in diffuse large B-cell lymphoma. *Haematologica* **103**, e215–e218 (2018).

137. Li, J. *et al.* Chimeric antigen receptor T cell (CAR-T) immunotherapy for solid tumors : lessons learned and strategies for moving forward. *J. Hematol. Oncol.* **11**, (2018).

138. Hege, K. M. *et al.* Safety , tumor trafficking and immunogenicity of chimeric antigen receptor (CAR)-T cells specific for TAG-72 in colorectal cancer. *J. Immunother. Cancer* **5**, (2017).

139. Guedan, S. *et al.* Enhancing CAR T cell persistence through ICOS and 4-1BB costimulation. *J. Clin. Investig. Insight* **3**, (2018).

140. Hay, K. A. & Turtle, C. J. Chimeric Antigen Receptor (CAR) T cells: Lessons Learned from Targeting of CD19 in B cell malignancies. *Drugs* **77**, 237–245 (2017).

141. Brentjens, R. J. *et al.* Safety and persistence of adoptively transferred autologous CD19-targeted T cells in patients with relapsed or chemotherapy refractory B-cell leukemias. *Blood* **118**, 4817–4828 (2011).

142. Mueller, S. N., Gebhardt, T., Carbone, F. R. & Heath, W. R. Memory T Cell Subsets , Migration Patterns, and Tissue Residence. *Annu Rev Immunol* **31**, 137–61 (2013).

143. Gargett, T. & Brown, M. P. Different cytokine and stimulation conditions influence the expansion and immune phenotype of third-generation chimeric antigen receptor T cells specific for tumor antigen GD2. *Cytotherapy* **17**, 487–495 (2015).

144. Lee, D. W. *et al.* Current concepts in the diagnosis and management of cytokine release syndrome. *Blood* **124**, 188–196 (2014).

145. Santomasso, B. D. *et al.* Clinical and Biological Correlates of Neurotoxicity Associated with CAR T Cell Therapy in Patients with B-cell Acute Lymphoblastic Leukemia (B-ALL). *Cancer Discov.* **8**, 958–971 (2018).

146. Lowe, K. L. *et al.* Fludarabine and neurotoxicity in engineered T-cell therapy. *Gene Ther.* **25**, 176–191 (2018).

147. Knochelmann, H. M. *et al.* CAR T Cells in Solid Tumors: Blueprints for Building effective Therapies. *Front. Immunol.* **9**, 1740 (2018).

148. Katz, S. C. *et al.* Phase I Hepatic Immunotherapy for Metastases study of intra-arterial chimeric antigen receptor modified T cell therapy for CEA+ liver metastases. *Clin. Cancer Res.* **21**, 3149–3159 (2015).

149. Ahmed, N. *et al.* Human Epidermal Growth Factor Receptor 2 (HER2) – Specific Chimeric Antigen Receptor – Modified T Cells for the Immunotherapy of HER2-Positive Sarcoma. *J. Clin. Oncol.* **33**, 1688–1696 (2015).

150. Rourke, D. M. O. *et al.* A single dose of peripherally infused EGFRvIII-directed CAR T cells mediates antigen loss and induces adaptive resistance in patients with recurrent glioblastoma. *Sci. Transl. Med.* **9**, (2017).

151. Maude, S. L. *et al.* Tisagenlecleucel in Children and Young Adults with B-Cell Lymphoblastic Leukemia. *N. Engl. J. Med.* **378**, 439–448 (2018).

152. D'Aloia, M. M., Zizzari, I. G., Sacchetti, B., Pierelli, L. & Alimandi, M. CAR-T cells: the long and winding road to solid tumors. *Cell Death Dis.* **9**, (2018).

153. Brown, C. E. *et al.* Bioactivity and Safety of IL13Ra2-Redirected Chimeric Antigen Receptor CD8+ T cells in Patients with Recurrent Glioblastoma. *Clin. Cancer Res.* **21**, 4062–4072 (2015).

154. Ahmed, N. *et al.* HER2-Specific Chimeric Antigen Receptor-Modified Virus-Specific T Cells for Progressive Glioblastoma. *JAMA Oncol* **3**, 1094–1101 (2017).

155. Chow, K. K. H. *et al.* T Cells Redirected to EphA2 for the Immunotherapy of Glioblastoma. *Mol. Ther.* **21**, 629–637 (2013).

156. Pellegatta, S. *et al.* Constitutive and TNFa-inducible expression of chondroitin sulfate proteoglycan 4 in glioblastoma and neurospheres : Implications for CAR-T cell therapy. *Sci. Transl. Med.* **10**, (2018).

157. Yi, Z., Prinzing, B. L., Cao, F., Gottschalk, S. & Krenciute, G. Optimizing EphA2-CAR T Cells for the Adoptive Immunotherapy of Glioma. *Mol. Ther. Methods Clin. Dev.* **9**, 70–80 (2018).

158. Bielamowicz, K. *et al.* Trivalent CAR T cells overcome interpatient antigenic variability in glioblastoma. *Neuro. Oncol.* **20**, 506–518 (2018).

159. Jiang, H. *et al.* Selective Targeting of Glioblastoma with EGFRvIII / EGFR Bitargeted Chimeric Antigen Receptor T Cell. *Cancer Immunol. Res.* **6**, 1314–1327 (2018).

160. Wang, D. *et al.* Glioblastoma-targeted CD4 + CAR T cells mediate superior antitumor activity. *J. Clin. Investig. Insight* **3**, (2018).

161. Brown, C. E. *et al.* Regression of Glioblastoma after Chimeric Antigen Receptor T-Cell Therapy. *N. Engl. J. Med.* **375**, 2561–2569 (2016).

162. Friedman, H. S. *et al.* Bevacizumab Alone and in Combination With Irinotecan in Recurrent Glioblastoma. *J. Clin. Oncol.* **27**, 4733–4740 (2009).

163. Kochenderfer, J. N. *et al.* Chemotherapy-refractory diffuse large B-cell lymphoma and indolent B-cell malignancies can be effectively treated with autologous T cells expressing an anti-CD19 chimeric antigen receptor. *J. Clin. Oncol.* **33**, 540–549 (2015).

164. Picarda, E., Ohaegbulam, K. C. & Zang, X. Molecular Pathways: Targeting B7-H3 (CD276) for Human Cancer Immunotherapy. *Clin. Cancer Res.* **22**, 3425–3431 (2016).

165. De Bacco, F. *et al.* The MET oncogene is a functional marker of a glioblastoma stem cell subtype. *Cancer Res.* **72**, 4537–4550 (2012).

166. Orzan, F. *et al.* Genetic Evolution of Glioblastoma Stem-Like Cells From Primary to Recurrent Tumor. *Stem Cells* **35**, 2218–2228 (2017).

167. Lee, J. *et al.* Tumor stem cells derived from glioblastomas cultured in bFGF and EGF more closely mirror the phenotype and genotype of primary tumors than do serum-cultured cell lines. *Cancer Cell* **9**, 391–403 (2006).

168. Du, H. *et al.* Antitumor Responses in the Absence of Toxicity in Solid Tumors by Targeting B7-H3 via Chimeric Antigen Receptor T Cells. *Cancer Cell* **35**, 221–237 (2019).

169. Diaconu, I. *et al.* Inducible Caspase-9 Selectively Modulates the Toxicities of CD19-Specific Chimeric Antigen Receptor-Modified T Cells. *Mol. Ther.* **25**, 580–592 (2017).

170. Pellegatta, S. *et al.* Neurospheres enriched in cancer stem-like cells are highly effective in eliciting a dendritic cell-mediated immune response against malignant gliomas. *Cancer Res.* **66**, 10247–10252 (2006).

171. Al-Hajj, M. Cancer stem cells and oncology therapeutics. *Curr. Opin. Oncol.* **19**, 61–64 (2007).

172. Esparza, R., Azad, T. D., Feroze, A. H., Mitra, S. S. & Cheshier, S. H. Glioblastoma stem cells and stem cell-targeting immunotherapies. *J. Neurooncol.* **123**, 449–457 (2015).

173. Brudno, J. N. & Kochenderfer, J. N. Toxicities of chimeric antigen receptor T cells: Recognition and management. *Blood* **127**, 3321–3330 (2016).

174. Kramer, K. *et al.* Compartmental intrathecal radioimmunotherapy: Results for treatment for metastatic CNS neuroblastoma. *J. Neurooncol.* **97**, 409–418 (2010).

175. Zhao, Z. *et al.* Structural Design of Engineered Costimulation Determines Tumor Rejection Kinetics and Persistence of CAR T Cells. *Cancer Cell* **28**, 415–428 (2015).

176. Finocchiaro, G. & Pellegatta, S. Immunotherapy with dendritic cells loaded with glioblastoma stem cells: from preclinical to clinical studies. *Cancer Immunol. Immunother.* **65**, 101–109 (2016).

177. Ramos, C. A. *et al.* Clinical responses with T lymphocytes targeting malignancy-associated κ light chains. *J. Clin. Invest.* **126**, 2588–2596 (2016).

178. Hong, L. K. *et al.* CD30-Redirected Chimeric Antigen Receptor T Cells Target CD30 + and CD30 − Embryonal Carcinoma via Antigen-Dependent and Fas/FasL Interactions . *Cancer Immunol. Res.* **6**, 1274–1287 (2018).

179. Anderson, K. G., Stromnes, I. M. & Greenberg, P. D. Obstacles posted by the tumor microenvironment to T cell activity: a case for synergistic therapies. *Cancer Cell* **31**, 311–325 (2017).